



Mobility & Vehicle Mechanics

*International Journal for Vehicle Mechanics, Engines and
Transportation Systems*

ISSN 1450 - 5304

UDC 621 + 629(05)=802.0

Mohamed Ali Emam	A NEW PROGRAM FOR PREDICTING OFF-ROAD VEHICLE MOBILITY	1-15
Dimitrios Koulocheris Georgios Papaioannou Dimitrios Christodoulou	ASSESSMENT OF THE OPTIMIZATION PROCEDURE FOR THE NON LINEAR SUSPENSION SYSTEM OF A HEAVY	17-35
Mikhail G. Shatrov Leonid N. Golubkov Andrey U. Dunin Pavel V. Dushkin	HYDRODYNAMIC EFFECTS IN COMMON RAIL FUEL SYSTEM IN CASE OF MULTIPLE INJECTION OF DIFFERENT FUELS	37-52
Vanja Šušteršič Dušan Gordić Mladen Josijević Vladimir Vukašinić	APPLICATION AND DESIGN OF HYDRO TRANSMISSION FOR TRACTORS	53-65
Nenad Kostić Nenad Marjanović Nenad Petrović	A NOVEL APPROACH FOR SOLVING GEAR TRAIN OPTIMIZATION PROBLEM	67-76



M V M

Mobility Vehicle Mechanics

Editors: Prof. dr Jovanka Lukić; Prof. dr Čedomir Duboka

MVM Editorial Board
University of Kragujevac
Faculty of Engineering
Sestre Janjić 6, 34000 Kragujevac, Serbia
Tel.: +381/34/335990; Fax: + 381/34/333192

Prof. Dr **Belingardi Giovanni**
Politecnico di Torino,
Torino, ITALY

Dr Ing. **Ćučuz Stojan**
Visteon corporation,
Novi Jicin,
CZECH REPUBLIC

Prof. Dr **Demić Miroslav**
University of Kragujevac
Faculty of Engineering
Kragujevac, SERBIA

Prof. Dr **Fiala Ernest**
Wien, OESTERREICH

Prof. Dr **Gillespie D. Thomas**
University of Michigan,
Ann Arbor, Michigan, USA

Prof. Dr **Grujović Aleksandar**
University of Kragujevac
Faculty of Engineering
Kragujevac, SERBIA

Prof. Dr **Knapezyk Josef**
Politechniki Krakowskiej,
Krakow, POLAND

Prof. Dr **Krstić Božidar**
University of Kragujevac
Faculty of Engineering
Kragujevac, SERBIA

Prof. Dr **Mariotti G. Virzi**
Universita degli Studidi Palermo,
Dipartimento di Meccanica ed
Aeronautica,
Palermo, ITALY

Prof. Dr **Pešić Radivoje**
University of Kragujevac
Faculty of Engineering
Kragujevac, SERBIA

Prof. Dr **Petrović Stojan**
Faculty of Mech. Eng. Belgrade,
SERBIA

Prof. Dr **Radonjić Dragoljub**
University of Kragujevac
Faculty of Engineering
Kragujevac, SERBIA

Prof. Dr **Radonjić Rajko**
University of Kragujevac
Faculty of Engineering
Kragujevac, SERBIA

Prof. Dr **Spentzas Constantinos**
N. National Technical University,
GREECE

Prof. Dr **Todorović Jovan**
Faculty of Mech. Eng. Belgrade,
SERBIA

Prof. Dr **Toliskyj Vladimir E.**
Academician NAMI,
Moscow, RUSSIA

Prof. Dr **Teodorović Dušan**
Faculty of Traffic and Transport
Engineering,
Belgrade, SERBIA

Prof. Dr **Veinović Stevan**
University of Kragujevac
Faculty of Engineering
Kragujevac, SERBIA

For Publisher: Prof. dr Miroslav Živković, dean, University of Kragujevac, Faculty of Engineering

*Publishing of this Journal is financially supported from:
Ministry of Education, Science and Technological Development, Republic Serbia*

Mobility &

Motorna

Vehicle

**Volume 42
Number 2
2016.**

Vozila i

Mechanics

Motori

Mohamed Ali Emam	A NEW PROGRAM FOR PREDICTING OFF-ROAD VEHICLE MOBILITY	1-15
Dimitrios Koulocheris Georgios Papaioannou Dimitrios Christodoulou	ASSESSMENT OF THE OPTIMIZATION PROCEDURE FOR THE NON LINEAR SUSPENSION SYSTEM OF A HEAVY VEHICLES	17-35
Mikhail G. Shatrov Leonid N. Golubkov Andrey U. Dunin Pavel V. Dushkin Andrey L. Yakovenko	HYDRODYNAMIC EFFECTS IN COMMON RAIL FUEL SYSTEM IN CASE OF MULTIPLE INJECTION OF DIFFERENT FUELS	37-52
Vanja Šušteršič Dušan Gordić Mladen Josijević Vladimir Vukašinović	APPLICATION AND DESIGN OF HYDRO TRANSMISSION FOR TRACTORS	53-65
Nenad Kostić Nenad Marjanović Nenad Petrović	A NOVEL APPROACH FOR SOLVING GEAR TRAIN OPTIMIZATION PROBLEM	67-76

Mobility &

Motorna

Vehicle

**Volume 42
Number 2
2016.**

Vozila i

Mechanics

Motori

Mohamed Ali Emam	NOVI PROGRAM ZA PREDVIĐANJE MOBILNOSTI TERENSKIH VOZILA	1-15
Dimitrios Koulocheris Georgios Papaioannou Dimitrios Christodoulou	OCENA PROCEDURE OPTIMIZACIJE NELINEARNOG SISTEMA OSLANJANJA TEŠKIH VOZILA	17-35
Mikhail G. Shatrov Leonid N. Golubkov Andrey U. Dunin Pavel V. Dushkin Andrey L. Yakovenko	HIDRODINAMIČKI EFEKTI KOD COMMON RAIL SISTEMA UBRIZGAVANJA GORIVA SA VIŠE BRIZGAČA RAZLIČITIH GORIVA	37-52
Vanja Šušteršič Dušan Gordić Mladen Josjević Vladimir Vukašinović	PRIMENA I PROJEKTOVANJE HIDRO TRANSMISIJA KOD TRAKTORA	53-65
Nenad Kostić Nenad Marjanović Nenad Petrović	NOVI PRISTUP REŠAVANJU OPTIMIZACIJE ZUPČASTIH PRENOSNIKA	67-76

A NEW PROGRAM FOR PREDICTING OFF-ROAD VEHICLE MOBILITY

Mohamed Ali Emam¹

UDC:629.016

ABSTRACT: An off-road vehicles` mobility program that predicts off-road vehicles mobility has been created to meet requirements for both research and educational programs. The program allows quick prediction of off-road vehicles` performance prior to their usage in sites as it checks whether soil properties are compatible with vehicles` parameters and configuration. The program also may be helpful in comparing and assessing the results of vehicles` mobility investigation obtained by using different methods and concluding the parameters affecting vehicles` mobility. The program has been written in Microsoft Visual Basic.net 2008 and can be considered as a new tool for predicting off-road vehicles` mobility. The program provides an intuitive user interface by linking databases such as off-road vehicles` specifications, soil parameters, and empirical equations to predict the wheel formula, motion resistance ratio, torque ratio, net traction ratio and the traction efficiency. It has been proven that the program is easily to use, simple, and efficient.

KEY WORDS: off-road vehicle mobility, wheel formula, motion resistance ratio, torque ratio, net traction ratio, tractive efficiency, simulation

NOVI PROGRAM ZA PREDVIĐANJE MOBILNOSTI TERENSKIH VOZILA

REZIME: Razvijeni program za predviđanje mobilnosti terenskih namenjen je za potrebe kako za istraživanja i za programe obrazovanja. On omogućava brzo predviđanje performansi terenskih vozila pre njihovog korišćenja na u eksploatacionim uslovima, tako što proverava da li su svojstva zemljišta kompatibilna sa parametrima vozila i konfiguracijom. Program takođe može biti od pomoći u poređenju i proceni rezultata mobilnosti vozila dobijenih korišćenjem različitih metoda i parametara koji utiču na mobilnost vozila. Napisan je u Microsoft Visual Basic.net 2008 i može se smatrati kao novo sredstvo za predviđanje mobilnosti terenskih vozila. Program nudi intuitivni korisnički interfejs povezivanjem baza podataka kao što su specifikacije vozila, parametri tla i empirijske jednačine za predviđanje numeričke formula točka, odnosa otpora kretanja, odnosa obrtnog momenta, neto odnosa vuče i efikasnosti vuče. Dokazano je da je program lak za korišćenje, da je jednostavan i efikasan.

KLJUČNE REČI: indeks mobilnosti terenskih vozila, formula točkova, koeficijent otpora kretanju, indeks obrtnog momenta, indeks vuče, efikasnost vuče, simulacija

¹ *Received: June 2016, Accepted July 2016, Available on line November 2016*

Intentionally blank

A NEW PROGRAM FOR PREDICTING OFF-ROAD VEHICLE MOBILITY

*Mohamed Ali Emam*¹

UDC:629.016

1. INTRODUCTION

Simulation programs and computer models for predicting off road vehicles` mobility help researchers to determine the relative importance of many factors affecting field mobility of off road vehicles without conducting expensive, as well as time consuming, field tests. They also help designers and researchers to develop and improve the off road vehicles` mobility by comparing and analysing various parameters that influence their mobility. The development of new software and programming languages always facilitate the use of computers in many different areas.

Actually, many conducted vehicles` mobility researches based on developing empirical equations exist. These equations can be adapted and used in the process of design and implementation of simulation programs both service educational and research needs in terra mechanics area.

The first steps in developing a method for off road vehicles` performance evaluation include tires` testing on natural terrain surfaces to develop linked vehicles` performance - terrain conditions. The analytical approach is concerned with predicting the performance of a traction device in terrain; in this regard, the distribution of normal and shear stress at the soil-tire/track interface and the geometry of the 3-D contact surface must be firstly determined. There are two other approaches; empirical and semi-empirical. The empirical approach is based on cone index results for predicting the off-road vehicles` mobility by using dimensionless tire performance coefficients; this is the main task of the present paper. The semi-empirical approach is usually involved in measuring soil deformation parameters, then calculating the soil shear-stress and deformation under a traction device that is assumed to be similar to generated shear by a torsion shear device. Bekker [1-2] assumed the normal stress under a flat plate depends on sinkage, plate width and soil coefficient.

Freitag [3] developed the first dimensionless wheel numeric and empirical mobility models based on wheel numeric. The wheel performance was measured at different weights on standard soils using soil bin and test lanes on terrain. Turnage [4-7] developed the method further, and presented separate mobility models dependent on soil properties for friction and cohesion soils. For cohesion soil the author used an average cone index, and a cone index gradient for the friction soils. Wismer & Luth [8] combined mobility models with soil shear model and included the slip into mobility models. This model became one kind of basic mobility model for several later researches. Gee-Glough [9-10] found out, that soil shear strength was somewhat correlated with penetration resistance, and added a soil shear factor into the model. Brixius [11-12] developed a more generalized expression for tractive characteristics of bias-ply pneumatic tires. The approach is based on a modified mobility number. Maclaurin [13-16] studied the influence of soil surface properties and tire patterns on wheel performance using WES-method as a frame of reference. Rowland [17],

¹ *Mohamed Ali Emam, Helwan University, Automotive and Tractor Engineering Dept., Faculty of Engineering – Mataria, P.O. Box 11718, Egypt, mohemam_70@yahoo.com*

Rowland and Peel [18], developed WES modelling depending on a new wheel numeric, and extended it also for tracked vehicles. The author presented the concept of mean maximum pressure MMP, which is the maximum allowable calculated soil contact pressure at a no-go situation. Several authors in different countries have used available models, or presented improved versions of empirical mobility models using penetrometer resistance as soil parameter.

The mobility of a vehicle is influenced by a lot of parameters which make the evaluation process complicated. Including more parameters in the evaluation process will probably give more accurate results, but it is not definitely true. However, accurate results will be expected if the included parameters are thoroughly analyzed and well assessed. The total vehicle mobility is influenced by many factors, as shown in the chart shown in Fig.1 [19].

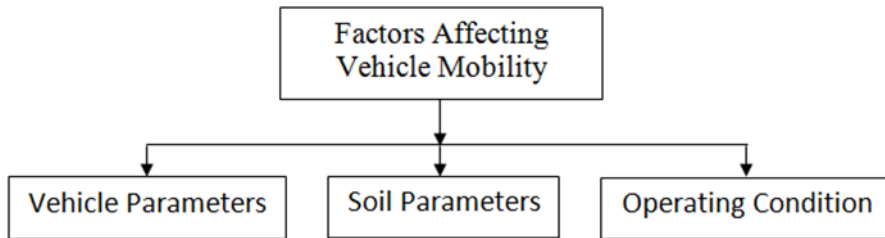


Figure 1 General scheme of factors affecting vehicle mobility [19]

The methods used to quantify off-road vehicles` mobility depend - to a large extent- on the purpose for which the vehicle is used; for military vehicles, the ability to traverse particular terrains and the speed with which this can be achieved are the most important aspects of performance while, for agricultural vehicles, the efficiency with which a task can be completed or the impact of the operation on the terrain may be of greater significance. The shift in emphasis between vehicle and terrain characteristics is often reflected in the terminology used: traffic-ability, for example, is defined as “the ability of a section of terrain to support mobility”, whereas mobility describes the efficiency with which a given vehicle can travel from one point to another across a given section of terrain [20]. Figure 2 presents an overview of the research interest, and illustrates the primary components of any predictive mobility modelling tool [20].

The aim of the paper was to develop a generalizing mobility program in Visual Basic.net 2008 as a new technique to that could be used to predict key measures of mobility such as wheel numeric, motion resistance ratio, torque ratio, net traction ratio and tractive efficiency, which can be used to represent off-road vehicles of varying parameters affected by different terrain (soil parameters).

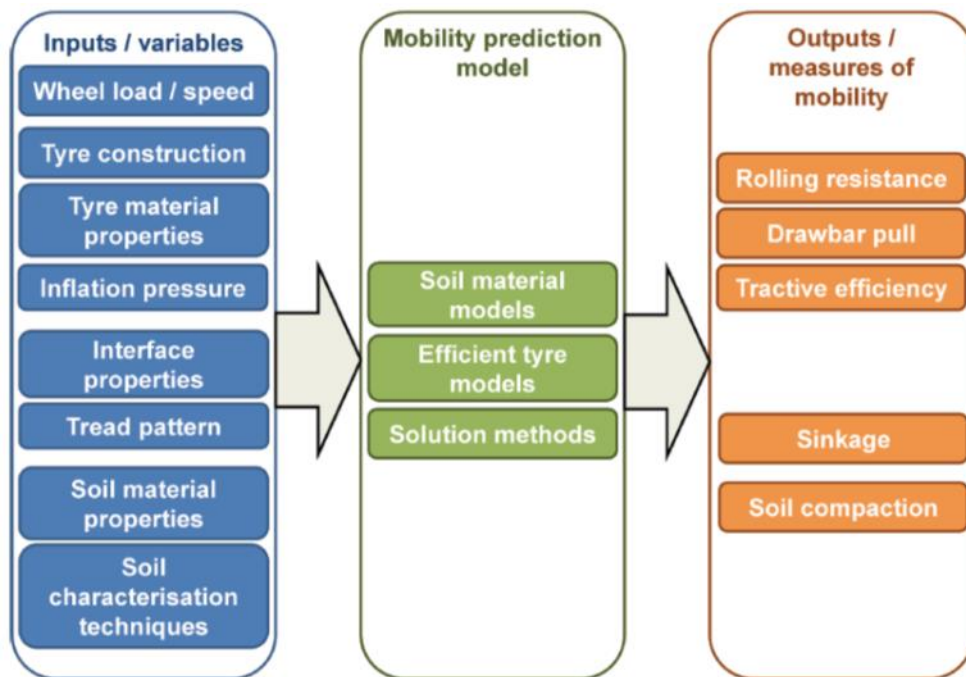


Figure 2 Overview of research interest [20]

2. OFF-ROAD VEHICLE MOBILITY EQUATIONS

The equations used to predict off-road mobility are numerous and depend on many parameters related to both vehicles and the terrains. In the following the mobility prediction equations have been used in developing the computer program.

2.1 Wheel numeric

The wheel numeric is a dimensionless variable calculated using a special formula, which includes tire and soil parameters. Different authors have proposed different empirical wheel numeric models for determining the best fitting combinations of tire dimensions and deflection with observed tire performance. The wheel numeric is defined in the Table 1 with different methods.

Table 1 Wheel numeric equations proposed by different researchers

No.	Method	Equation
1	Wisner & Luth [8]	$C_n = \frac{CI b d}{W} \quad (1)$
2	Freitage [3]	$N_C = \frac{CI b d}{W} \sqrt{\frac{\delta}{h}} \text{ for clay, and } N_S = \frac{G (b.d)^{3/2}}{W} \cdot \frac{\delta}{h} \text{ for sand} \quad (2)$
3	Turnage [4-7]	$N_{CI} = \frac{CI b d}{W} \sqrt{\frac{\delta}{h}} \cdot \frac{1}{1 + \frac{b}{2.d}} \quad (3)$
4	Brixius [11-12]	$B_n = \frac{CI b d}{W} \left(\frac{1 + \frac{5\delta}{h}}{1 + \frac{3b}{d}} \right) \quad (4)$
5	Rowland & Peel [18]	$N_R = \frac{CI \cdot b^{0.85} \cdot d^{1.15}}{W} \sqrt{\frac{\delta}{h}} \quad (5)$
6	Maclaurin [13-16]	$N_m = \frac{CI \cdot b^{0.8} d^{0.8} \delta^{0.4}}{W} \quad (6)$

2.2 Motion resistance ratio, (μ_{mrr})

The general equation of the motion resistance ratio is written as:

$$\mu_{mrr} = \frac{RR}{W} \quad (7)$$

The motion resistance ratio is a dimensionless variable calculated by using wheel numeric formulas proposed by various researchers, this is shown in Table 2.

Table 2 Motion resistance ratio equations proposed by various researchers

No.	Method	Equation
1	Wisner & Luth [8]	$\mu_{mrr(Wisner \& Luth)} = \frac{1.2}{C_n} + 0.04 \quad (8)$
2	Freitage [3]	$\mu_{mrr(Freitage)} = \frac{1.2}{N_S} + 0.04 \quad (9)$
3	Turnage [4-7]	$\mu_{mrr(Turnage)} = 0.04 + \frac{0.2}{N_{CI} - 2.5} \quad (10)$
4	Brixius [11-12]	$\mu_{mrr(Brixius)} = \frac{1}{B_n} + \frac{0.5 s}{\sqrt{B_n}} + 0.04 \quad (11)$
5	Rowland & Peel [18]	$\mu_{mrr(Rowland \& Peel)} = 3 (1 + S) N_R^{-2.7} \quad (12)$
6	Maclaurin [13-16]	$\mu_{mrr(Maclaurin)} = 0.017 + \frac{0.435}{N_{CI}} \quad (13)$

7	Ashmore [21]	$\mu_{mrr(Ashmore)} = -0.1\left(\frac{W}{W_r}\right) + \frac{0.22}{C_n} + 0.2$	(14)
8	Gee-Glough [9-10]	$\mu_{mrr(Gee-Glough)} = 0.049 + \frac{0.287}{N_{Cl}}$	(15)
9	Dwyer [22-23]	$\mu_{mrr(Dwyer)} = 0.05 + \frac{0.287}{N_{Cl}}$	(16)

The third mechanism, based on both geometry and the effect of local deformities, is the transformation of sharp, singular edges of the observed unevenness into smooth segments of the enveloping curve.

2.3 Torque ratio, (μ_{tr})

The general equation of the torque ratio is written as:

$$\mu_{tr} = \frac{T}{r * W} \tag{17}$$

The torque ratio is a dimensionless variable calculated using wheel numeric formulas proposed by various researchers, this shown in Table 3.

Table 3 Torque ratio equations

No.	Method	Equation	
1	Wismer & Luth [8]	$\mu_{tr(Wismer \& Luth)} = 0.75 (1 - e^{-0.3C_n s})$	(18)
2	Freitage [3]	$\mu_{tr(Freitage)} = 0.75 (1 - e^{-0.3N_s s})$	(19)
4	Brixius [11-12]	$\mu_{tr(Brixius)} = 0.88 (1 - e^{-0.1B_n})(1 - e^{-0.75s}) + 0.04$	(20)
7	Ashmore [21]	$\mu_{tr(Ashmore)} = 0.47 (1 - e^{-0.2C_n s}) + 0.28\left(\frac{W}{W_r}\right)$	(21)
9	Dwyer [22-23]	$\mu_{tr(Dwyer)} = 0.796 - \frac{0.92}{N_{Cl}}$	(22)

2.4 Net traction ratio, (μ_{ntr})

The general equation of the net traction ratio is written as:

$$\mu_{ntr} = \frac{NT}{W} = \mu_{tr} - \mu_{mrr} \quad (23)$$

The various net traction ratios are given in Table 4.

Table 4 Equations for traction ratio

No.	Method	Equation	
1	Wisner & Luth [8]	$\begin{aligned} \mu_{ntr(Wisner \& Luth)} \\ = \mu_{tr(Wisner \& Luth)} \\ - \mu_{mrr(Wisner \& Luth)} \end{aligned}$	(24)
2	Freitage [3]	$\mu_{ntr(Freitage)} = \mu_{tr(Freitage)} - \mu_{mrr(Freitage)}$	(25)
4	Brixius [11-12]	$\mu_{ntr(Brixius)} = \mu_{tr(Brixius)} - \mu_{mrr(Brixius)}$	(26)
5	Rowland & Peel [18]	$\mu_{ntr(Rowland \& Peel)} = 0.12 N_R^{0.88} (1 - 0.61(1 - S)^4)$	(27)
6	Maclaurin [13-16]	$\mu_{ntr(Maclaurin)} = 0.817 - \frac{3.2}{N_{Cl} + 1.91} + \frac{0.453}{N_{Cl}}$	(28)
7	Ashmore [21]	$\mu_{ntr(Ashmore)} = \mu_{tr(Ashmore)} - \mu_{mrr(Ashmore)}$	(29)
8	Gee-Glough [9-10]	$\mu_{ntr(Gee-Glough)} = \mu_{ntr_{max}} (1 - e^{-ks})$	(30)
9	Dwyer [22-23]	$\begin{aligned} \mu_{ntr(Dwyer)} = \\ \left(0.796 - \frac{0.92}{N_{Cl}}\right) \cdot (1 - e^{-(4.838+0.061 \cdot N_{Cl}) \cdot S}) \text{ at } 20\% \text{ wheel} \\ \text{slip} \end{aligned}$	(31)

2.5 Tractive efficiency, (TE)

The general equation of the traction efficiency is written as:

$$TE = \left[\frac{\frac{NT}{W}}{\frac{T}{r \cdot W}} \right] (1 - s) = \frac{\mu_{ntr}}{\mu_{tr}} (1 - s) \quad (32)$$

Table 5 shows the equations for traction efficiency ratio.

Table 5 Tractive efficiency equations

No.	Method	Equation	
1	Wisner & Luth [8]	$TE_{(Wisner \& Luth)} = \frac{\mu_{ntr(Wisner \& Luth)}}{\mu_{tr(Wisner \& Luth)}} (1 - s)$	(33)
2	Freitage [3]	$TE_{(Freitage)} = \frac{\mu_{ntr(Freitage)}}{\mu_{tr(Freitage)}} (1 - s)$	(34)
4	Brixius [11-12]	$TE_{(Brixius)} = \frac{\mu_{ntr(Brixius)}}{\mu_{tr(Brixius)}} (1 - s)$	(35)
7	Ashmore [21]	$TE_{(Ashmore)} = \frac{\mu_{ntr(Ashmore)}}{\mu_{tr(Ashmore)}} (1 - s)$	(36)
8	Gee-Glough [9-10]	$TE_{(Gee-Glough)} = \frac{\mu_{ntr(Gee-Glough)}}{\mu_{tr(Gee-Glough)}} (1 - s)$	(37)
9	Dwyer [22-23]	$TE_{(Dwyer)} = \frac{\mu_{ntr(Dwyer)}}{\mu_{tr(Dwyer)}} (1 - s)$	(38)

3. OFF-ROAD VEHICLES` MOBILITY PREDICTION PROGRAM

A mobility software program has been fully created using Microsoft Visual Basic.net 2008. This is designed to calculate and plot the following; the wheel numeric, the motion resistance ratio, the torque ratio, the net traction ratio, and the traction efficiency.

Mobility contains several forms to calculate and plot the above mentioned equations every form contains easy ways to enter values of the equation. Then the mobility parameter is plotting chart of the equation using Microsoft .NET framework 3.5.1 and MSChart. It can compare the charts for each change of the values and use all functions of Microsoft Visual Basic.net 2008 (in the program) to modify the chart such as (chart name, Chart axis, etc.)

The MSChart control allows plotting data in charts according to any specifications. It can create a chart by setting data in the controls` properties page, or by retrieving data to be plotted from another source, such as a Microsoft Excel spread sheet. The information in this topic focuses on using an Excel worksheet as a data source. Figure 3 illustrates the relationship between the three programs and the role of each.

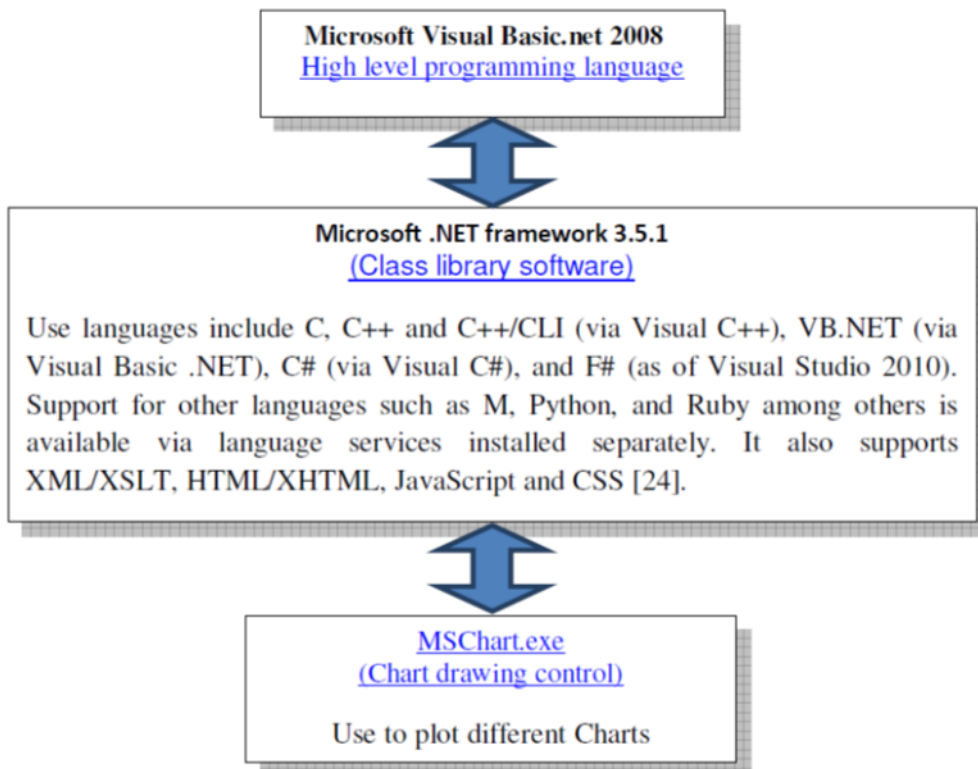


Figure 3 Relationship between the three programs and the role of each

The mobility program starts with an opening screen as shown in Fig. 4. The program mainly consists of two main sections, constant parameters and calculations menu as shown in Fig. 5. Each section has a number of subsections based on the design criteria for the program development. In the first section all constant parameters should be inserted. In the second section selection of calculation methods has to be done and plotting graphs with entering the variable parameters such as weight on tire, tire section width, overall tire diameter, tire section height, cone index and cone index gradient. The screen consists of five tabs (wheel numeric, motion resistance ratio, torque ratio, net traction ratio and traction efficiency), this helps in evaluating and comparing vehicles` mobility by using different methods as previously mentioned. The flow diagram of the program simulation part is shown in Fig. 6.



Figure 4 The opening screen of the mobility program

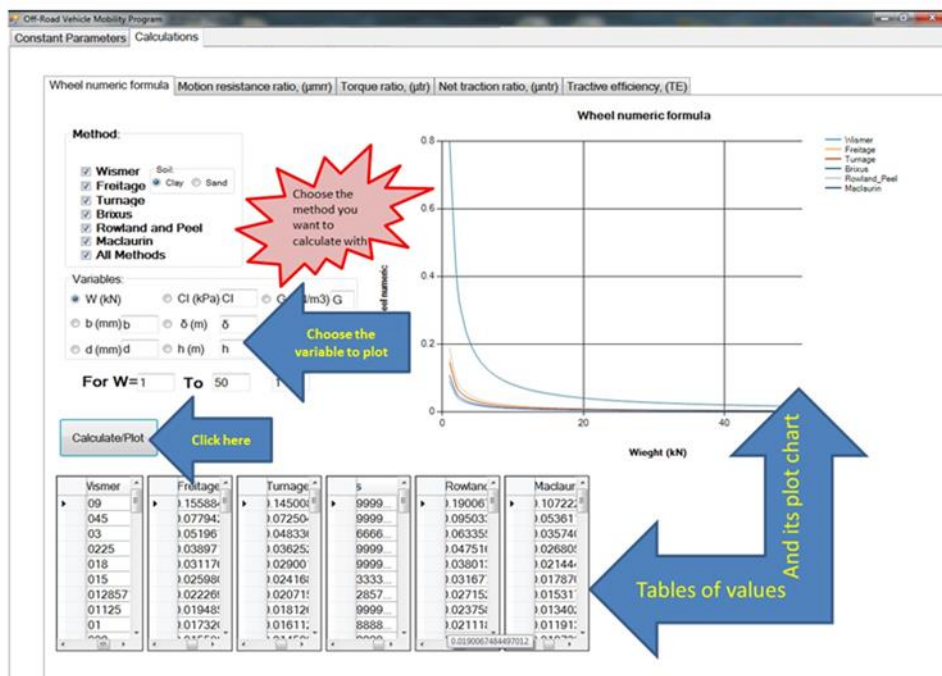


Figure 5 The calculation methods and plotting the relationships in the chart screen

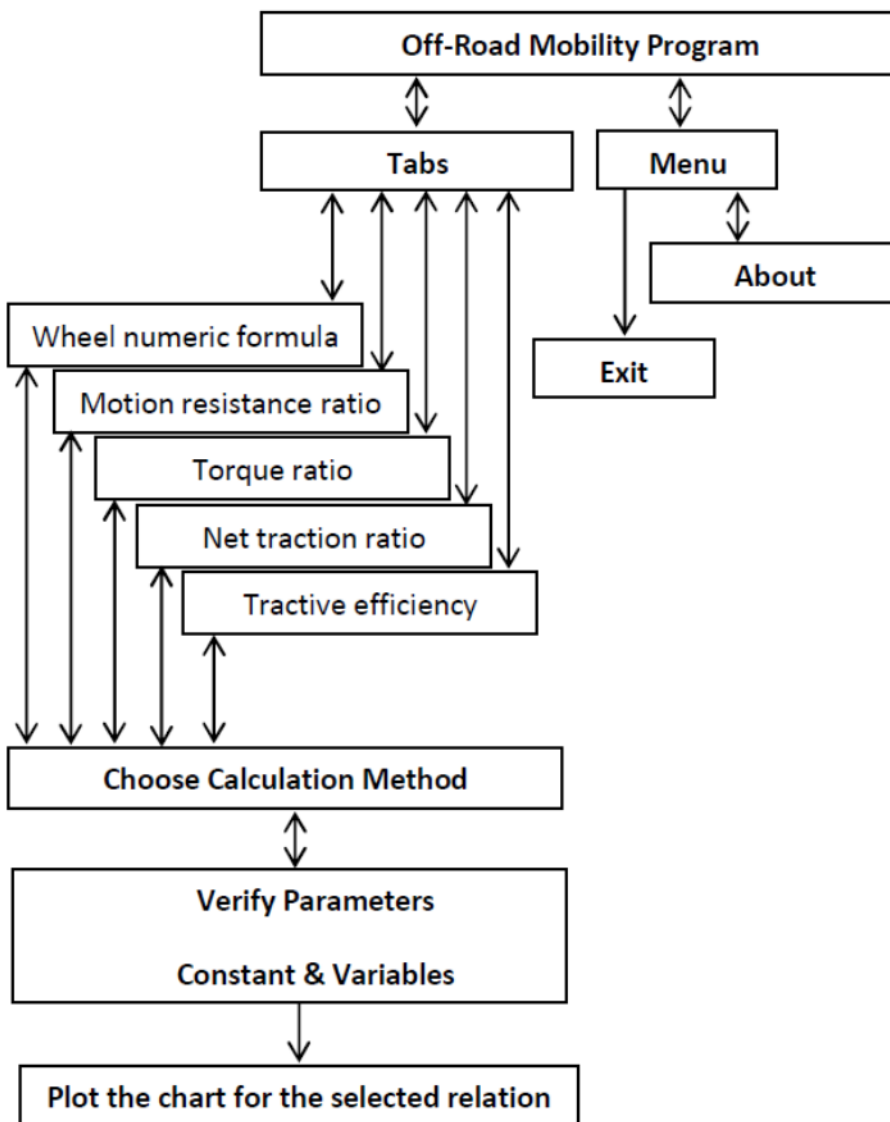


Figure 6 Flow diagram of Off-Road Mobility Program

The prediction equations of Wismer & Luth [8], Freitage [3], Turnage [4-7], Brixius [11-12], Rowland & Peel 18], Maclaurin [13-16], Ashmore [21], Gee-Glough [9-10], and Dwyer [22-23] were used in the computer model development for predicting the off-road vehicles` mobility. To validate the model, predicted mobility variables were compared against results, same numerical values were obtained for mobility variables. Samples of results from the program of the various parameters of predicting vehicles` mobility are shown in Figures 7 and 8.

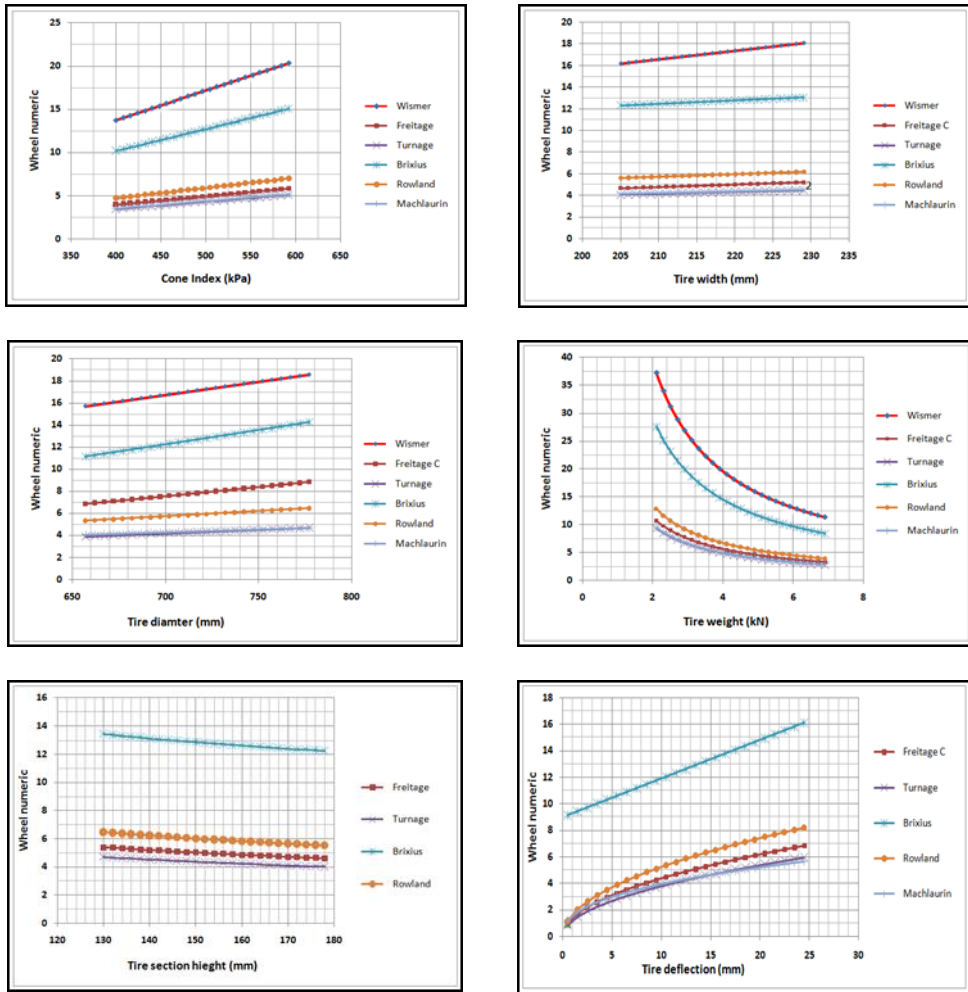


Figure 7 Variation of wheel numeric with soil cone index, tire width, tire diameter, tire weight, tire section height and tire deflection

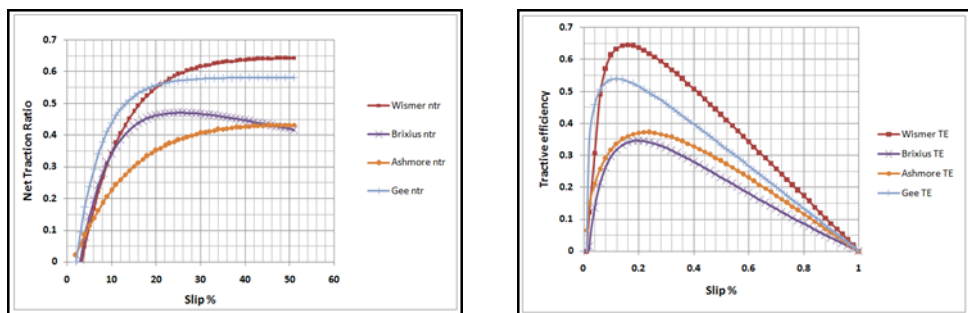


Figure 8 Variation of net traction ratio and traction efficiency with slip

4. CONCLUSION

A Microsoft Visual Basic.net 2008 programming for predicting off-road vehicles` mobility has been created; this program can be used for educational and research purposes. The program uses some empirical equations proposed by various researchers in the terrain-vehicle system area. The items in menus and object driven windows were vital in making the program relatively easy to learn and operate compared to the programs developed using any software tool available prior to the visual programming tools. The intuitive user interface to the model is a visual object-oriented window, which allows the selection of the off-road vehicle mobility parameters, the prediction method, the vehicles` specifications, the terrains` parameters, and the simulation. It can also access other windows to edit or expand available databases. These features provided by the facilities of visual programming make the program sufficiently flexible and interactive to the users in both research and education in terra mechanics area. The program has been proven to be easily using, simple, and efficient.

ACKNOWLEDGMENTS

The author thanks from his heart Prof. Dr. S. Shaaban in Automotive & Tractor Engineering Dept., Mataria Engineering, Helwan University, Egypt, for his kind advice and support.

REFERENCES

- [1] Bekker M G. Off-the-road locomotion. Research and development in terramechanics. University of Michigan Press, Ann Arbor. 220 s, 1960.
- [2] Bekker M G. Introduction to terrain-vehicle systems. University of Michigan Press, Ann Arbor. 846 s, 1969.
- [3] Freitag D R. A dimensional analysis of performance of pneumatic tires in soft soils. WES Technical report No3-688, 1965.
- [4] Turnage G W. Tire selection and performance prediction for off-road wheeled-vehicle operations. Proceedings of the 4th International ISTVS Conference, Stockholm-Kiruna, Sweden, April 24-28, 1972. I:62- 82, 1972.
- [5] Turnage G W. Using dimensionless prediction terms to describe off-road wheel vehicle performance. ASAE Paper No. 72-634, 1972 b.
- [6] Turnage G W. A synopsis of tire design and operational considerations aimed at increasing in soil tire drawbar performance. Proceedings of the 6th International ISTVS Conference, Vienna, Austria, August 22-25, 1978, II: 757-810, 1978.
- [7] Turnage G W. Prediction of in-sand tire and wheeled vehicle drawbar performance. Proceedings of the 8th International ISTVS Conference, Cambridge, UK, 6-10 July 1984, I: 121-150, 1984.
- [8] Wismer R D and Luth H J. Off-road traction prediction for wheeled vehicles. Transaction ASAE 17(1):8-10.14, 1973.
- [9] Gee-Clough D. A comparison of the mobility number and Bekker approaches to the traction mechanics and recent advances in both methods at the N.I.A.E. Proceedings of the 6th International ISTVS conference, Vienna, Austria, August 22-25, 1978. II: 735-755, 1978.

- [10] Gee-Clough D. Selection of tire sizes for agricultural vehicles. *Journal of agricultural engineering research* 25(3):261-278, 1980.
- [11] Brixius W W. Traction prediction equations for bias ply tires. ASAE paper No 87-1622, 1987.
- [12] Brixius W W and Wismer R D. Traction prediction for wheeled vehicles. John Deere Report No109, 1975.
- [13] Maclaurin E B. The effect of tread pattern on the field performance of tires. Proceedings of the 7th International ISTVS Conference, August 16-20. 1981, Calgary, Canada. II: 699-735, 1981.
- [14] Maclaurin E B. The use of mobility numbers to describe the in-field tractive performance of pneumatic tires. Proceedings of the 10th International ISTVS Conference, Kobe, Japan, August 20-24, 1990. I: 177-186, 1990.
- [15] Maclaurin E B. The use of mobility numbers to predict the tractive performance of wheeled and tracked vehicles in soft cohesive soils. Proceedings of the 7th European ISTVS Conference, Ferrara, Italy, 8-10. October 1997:391-398, 1997.
- [16] Maclaurin E B. Comparing the NRMM (VCI), MMP and VLCI traction models. *Journal of Terramechanics* 43–51, 2007.
- [17] Rowland D. Tracked vehicle ground pressure and its effect on soft ground performance. Proceedings of the 4th International ISTVS Conference April 24-28.1972, Stockholm-Kiruna, Sweden. I: 353-384, 1972.
- [18] Rowland D and Peel J W. Soft ground performance prediction and assessment for wheeled and tracked vehicles. *Institute of mechanical engineering* 205:81, 1975.
- [19] Yong R N., Ezzat A F and Nicolas S. *Vehicle Traction Mechanics*. ISBN 0-444-42378-8 (vol. 3), ISBN 0-444-41940-3 (Series), Elsevier Science Publishers B. V., 1984.
- [20] Andy W. Tire/soil interaction modelling within a virtual proving ground environment. PhD Thesis, Cranfield University, 2012.
- [21] Ashmore C, Burt C and Turner J. An empirical equation for predicting tractive performance of log skidder tires. *Transactions of the ASAE*, 30(5):1231-1236, 1987.
- [22] Dwyer M J. Tractive performance of a wide, low-pressure tire compared with conventional tractor drive tires. *Journal of terramechanics* 24(3):227-234, 1987.
- [23] Dwyer M J. Tractive performance of wheeled vehicles. *Journal of Terramechanics* 21(1):19-34, 1984.
- [24] Online, http://en.wikipedia.org/wiki/Microsoft_Visual_Studio
- [25] Online, <http://msdn.microsoft.com/en-us/library/ms123401.aspx>
- [26] Online, <http://www.tutorialspoint.com/vb.net/>

Intentionally blank

ASSESSMENT OF THE OPTIMIZATION PROCEDURE FOR THE NON LINEAR SUSPENSION SYSTEM OF A HEAVY VEHICLES

Dimitrios V. Koulocheris¹, Georgios D. Papaioannou and Dimitrios A. Christodouls

UDC:629.019

ABSTRACT: Suspension systems of vehicles influence the overall performance of the vehicle by receiving the loads created by the road. In the past, researchers introduced many types of suspension systems studying them with the use of vehicle models, such as passive, active, semi-active etc. Many studies turned their attention to the optimization of the suspension systems, so as to facilitate the influence of design parameters in order to get the minimum or the maximum of an objective function. This allowed researchers to investigate ways to combine important parameters of a vehicle in the objective function, so as to achieve the optimum combination of its important parameters, such as the ride comfort and the road holding; the most common trade off in the automotive industry. In this paper, not only the efficiency of different optimization methods is investigated but also the efficiency of various fitness and objective functions so as to achieve the optimum result in the dynamical behaviour of a heavy vehicle model.

KEY WORDS: optimization, suspension system, genetic algorithms, hybrid algorithm

OCENA PROCEDURE OPTIMIZACIJE NELINEARNOG SISTEMA OSLANJANJA TEŠKIH VOZILA

REZIME: Sistemi elastičnog oslanjanja vozila utiču na ukupne performanse vozila u toku primanja opterećenja nastalih na putu. U prošlosti, istraživači su uveli mnoge tipove sistema elastičnog oslanjanja proučavajući ih u upotrebi modela vozila, kao što su pasivni, aktivni, poluaktivni i drugi. Mnoge studije, okreću svoju pažnju optimizaciji sistema elastičnog oslanjanja, kako bi se olakšao uticaj projektnih parametara u cilju dobijanja minimuma ili maksimuma funkcije cilja. Ovo je omogućilo istraživačima da istraže načine kombinovanja važnih parametara vozila funkcije cilja, kako bi se postigla optimalna kombinacija tih važnih parametara, kao što su udobnost u vožnji i držanje na putu; najčešći kompromis u automobilskoj industriji. U ovom radu, nije samo istražena efikasnost različitih metoda optimizacije već i efikasnost raznih pogodnosti i funkcija cilja kako bi se postigao optimalni rezultat u dinamičkm ponašanju modela teških vozila.

KLJUČNE REČI: optimizacija, sistem elastičnog oslanjanja, genetski algoritmi, hibridni algoritam

¹ Received: July 2016, Accepted September 2016, Available on line November 2016

Intentionally blank

ASSESSMENT OF THE OPTIMIZATION PROCEDURE FOR THE NONLINEAR SUSPENSION SYSTEM OF A HEAVY VEHICLE

Dimitrios V. Koulocheris¹, Georgios D. Papaioannou², Dimitrios A. Christodoulou³

UDC:629.019

1. INTRODUCTION

Suspension systems influence the overall performance of the vehicle by receiving the loads created by the road excitation. These loads are transmitted through the tires and the wheels ensuring that vibrations are isolated and not perceived by the passengers. Depending on the aspect of interest regarding the design of a suspension system, the focus of the studies is turned on the ride comfort or the road holding of the vehicle being the basic needs for a good suspension system. Ride comfort is related to the passenger's perception of the moving vehicle's environment, while road holding is the degree to which a car maintains contact with the road surface in various types of directional changes. Keeping the tires in contact with the ground constantly is of vital importance for the friction between the vehicle and the road affecting the vehicle's ability to steer, brake and accelerate. Time domain statistics, such as mean suspension deflection, maximum and RMS values of suspension acceleration are often used in suspension design as criteria for road comfort ability. The main conflict and common trade-off in the automotive industry is the one concerning the displacement and the acceleration of the suspension. A hard configuration with high spring stiffness and high damping is required for reducing the suspension displacement. On the other hand, low spring stiffness and low damping is required for reducing suspension acceleration. This conflict depicts the trade-off between the ride comfort and the road holding.

Multibody dynamics have been used extensively by automotive industry to model and design vehicle suspension. Before modern optimization methods were introduced, design engineers used to follow the iterative approach of testing various input parameters for vehicle suspension performance, setting as targets predefined performance indexes so as to be achieved. With the advent of various optimization methods along with developments in computational studies, the design process has been speeded up to reach to optimal values of the design parameters. Many studies, turned their attention to the optimization of the suspension systems, so as to facilitate the influence of design parameters in order to get the minimum or the maximum of an objective function subjected to certain constraints. These constraints depicted the practical considerations into the design process.

The issue of the most appropriate objective function is the main subject of intense studies in order to be able to combine many aspects of the dynamical behaviour and overcome the aforementioned conflict of ride comfort and road holding. Georgiou et al [1].

Used a sum of the variances of the body acceleration, the suspension travel and the one of the tire forces as a fitness function. On the other hand, Ozcan et al. [2] used as fitness

¹ *Dimitrios V. Koulocheris, Assistant Professor, School of Mechanical Engineering, National Technical University of Athens, Heroon Polytechniou 9, Zografou, 15780 dbkoulva@central.ntua.gr*

² *Georgios D. Papaioannou, PhD Student, School of Mechanical Engineering, National Technical University of Athens, gpapaioan@central.ntua.gr*

³ *Dimitrios A. Christodoulou, Student, School of Mechanical Engineering, National Technical University of Athens, dchristodoulou0@gmail.com*

function the sum of the RMS value of the weighted body acceleration and the difference between the maximum and the minimum force applied to the tire. While Shirahatt et al. [3] selected the root mean square of the passenger's acceleration. Another index of performance was proposed by Gündoğdu et al [4], examining also the effect that the vehicle has on the passenger's body by adding to the fitness function, terms concerning the variance of the head's acceleration and the crest factor. Another approach regarding the fitness function included the use of the constraints as terms in the fitness function with suitable weights [5], depending on the importance of each constraint or as separate functions to the optimization algorithm [3]. This approach was followed also by Koulocheris et al. [6], where the maximum value of vertical acceleration of the vehicle body at the passenger seat was minimized from the view point of ride comfort adding a quadratic penalty of the sum of constraints functions.

In this paper the optimization of a suspension system is studied. More specifically, not only the efficiency of different methods is investigated but also the efficiency of various fitness and objective functions. Three optimization methods were used: Genetic Algorithms, Gradient Based and a hybridization of the above algorithms. In conclusion this paper is organized as follows: in Section 1 the model used for the optimization of the heavy vehicle is described as well as the road excitation applied, in Section 2 the methods are presented while in Section 3, the optimization procedure applied in the problem is analysed, in Section 4 and 5 the results of the current study are illustrated and discussed, and finally in Section 5 conclusions and future work are displayed.

2. VEHICLE MODEL

In this paper, a heavy vehicle was modelled as a Half Car Model, as shown in figure 1, so as to examine the vertical vibrations that are induced from the road. This model simulates the front and rear axle of the vehicle and it allows the pitch phenomena to be observed.

2.1 Equations of motion

The mass of the body of the vehicle is considered as a rigid bar. The body of the vehicle has a mass m_s , which is half of the total body mass, and lateral moment of inertia I_z , which is the half of the total body mass moment of inertia. The unspring masses for the front and rear wheel are m_F and m_R , respectively. The distance of the front and rear axle from the center of mass are a_F and a_R , respectively (Figure 1). Moreover, the tires are modelled with a spring system indicated by different parameters for the front and rear tires K_{TF} and K_{TR} , respectively and were evaluated experimentally on previous work [9]. The tires receive as input the road excitations, $Z_{Road F}$ and $Z_{Road R}$, which will be described in the next subchapter. The parameters of the vehicle are displayed in Tables 1 and 2.

A suspension system has to adjust to the irregularities of the road surface, in order to ensure the comfort of the passengers and the holding of the vehicle. This adjustment is related to certain nonlinearities in the main components of the suspension, which can be observed mostly in active suspension systems. But nonlinearities can be found in passive suspension systems too, with the addition of nonlinear terms in either the springs or the dampers of the suspension. In this work, the nonlinearity of the suspension spring is studied. The spring suspension force can be mathematically described as:

$$F_{spring} = K_l \cdot x + K_{nl} \cdot x^3 \quad (1)$$

Table 1 Parameters of Half Car Model

Values of Vehicle Parameters	
$m_s=2220$ [kg]	
$I_z = 1142$ [kg m ²]	
$m_F=50$ [kg]	$m_R=100$ [kg]
$a_F=1.61$ [m]	$a_R=1.67$ [m]
$K_{TF}=4*10^5$ [N/m]	$K_{TR} = 2K_{TF}$

Table 2 Nomenclature of Vehicle Parameters

Parameters		Subscripts	
z	Vertical motion coordinate	S	Body
θ	Pitch motion coordinate	F	Front
z _{Road}	Road excitation	R	Rear
m	Mass	l	Linear
C	Damper's coefficient	nl	Non-linear
K	Spring's stiffness coefficient	T	Tire
a	Distance of the center of mass of the vehicle		

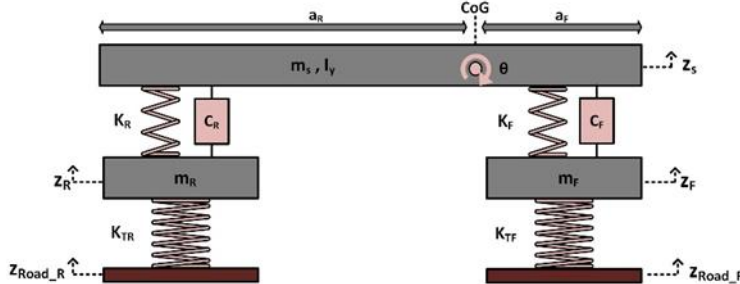


Figure 1 Half Car Model

The derivation of the equations is based on rigid body theory and on the assumption of small angles; $\sin\theta$ and $\cos\theta$ are approximated as θ and 1, respectively. Thus, the governing equations of the model are:

Body Bounce:

$$\begin{aligned}
 m_s \cdot \ddot{z}_s + C_F \cdot (\dot{z}_s - \dot{z}_F - a_F \cdot \dot{\theta}) + C_R \cdot (\dot{z}_s - \dot{z}_R + a_R \cdot \dot{\theta}) \\
 + K_{lF} \cdot (z_s - z_F - a_F \cdot \theta) + K_{lR} \cdot (z_s - z_R + a_R \cdot \theta) \\
 - K_{nlF} \cdot (z_s - z_F - a_F \cdot \theta)^3 + K_{nlR} \cdot (z_s - z_R + a_R \cdot \theta)^3 = 0
 \end{aligned}
 \tag{2}$$

Body Pitch:

$$\begin{aligned}
& I_z \cdot \ddot{\theta} - \alpha_F \cdot C_F \cdot (\dot{z}_S - \dot{z}_F - a_F \cdot \dot{\theta}) + \alpha_2 \cdot C_R \cdot (\dot{z}_S - \dot{z}_R + a_R \cdot \dot{\theta}) \\
& - \alpha_F \cdot K_{lF} \cdot (z_S - z_F - a_F \cdot \theta) + \alpha_2 \cdot K_{lR} \cdot (z_S - z_R + a_R \cdot \theta) \\
& - \alpha_F \cdot K_{nlF} \cdot (z_S - z - a_F \cdot \theta)^3 + \alpha_2 \cdot K_{nlR} \cdot (z_S - z_R + a_R \cdot \theta)^3 = 0
\end{aligned} \tag{3}$$

Front Wheel Bounce:

$$\begin{aligned}
& m_F \cdot \ddot{x}_F - C_F \cdot (\dot{z} - \dot{z}_F - a_F \cdot \dot{\theta}) - K_{lF} \cdot (z_S - z_F - a_F \cdot \theta) \\
& - K_{nlF} \cdot (z_S - z_F - a_F \cdot \theta)^3 + K_{TF} \cdot (z_F - z_{RoadF}) = 0
\end{aligned} \tag{4}$$

Rear Wheel Bounce:

$$\begin{aligned}
& m_R \cdot \ddot{x}_R - C_R \cdot (\dot{x}_S - \dot{x}_R + a_R \cdot \dot{\theta}) - K_{lR} \cdot (x_S - x_R + a_R \cdot \theta) \\
& - K_{nlR} \cdot (z_S - z_R + a_R \cdot \theta)^3 + K_{TR} \cdot (x_R - z_{RoadR}) = 0
\end{aligned} \tag{5}$$

One of the most important parameters of a vehicle model are the suspension travel as well as the tire deflection. The suspension travel of the suspension is the term $(z_S - z_R - a_R \cdot \theta)$ and $(z_S - z_R - a_R \cdot \theta)$ for the front and rear suspension respectively and the tire deflection is $(z_F - z_{RoadF})$ and $(z_R - z_{RoadR})$ for the front and rear tire respectively.

2.2 Road Excitation

Generally, the subject of road excitation is important, since it allows researchers to investigate realistic road profiles through simulation. In this study, a road bump was generated mathematically, with a half-sinusoid excitation function. The height of the bump was selected as $h=0.05$ m with an appropriate length for the half-sinusoid of $L=2$ m. The vehicle velocity was constant and at 10 m/s. As a function of time, the road conditions could be given by:

$$y_F = \begin{cases} h \cdot \sin(w \cdot t), & \text{if } t_0 \leq t < t_0 + \frac{L}{2 \cdot V} \\ 0, & \text{otherwise} \end{cases} \tag{6}$$

$$y_R = \begin{cases} h \cdot \sin(w \cdot t), & \text{if } t_0 + t_{distance} \leq t < t_0 + \frac{L}{2 \cdot V} + t_{distance} \\ 0, & \text{otherwise} \end{cases} \tag{7}$$

where t_0 is the starting time of the road bump, $t_{distance}$ is the time lag between front and rear wheels ($\frac{a_F + a_R}{V}$), whilst w is the excitation frequency $\frac{2 \cdot \pi \cdot L}{V}$. More specifically, the front and rear wheels follow the same trajectory with a time delay $t_{distance}$, which is due to the distance $a_F + a_R$ of front and rear wheels. The excitation is illustrated in Figure 2.

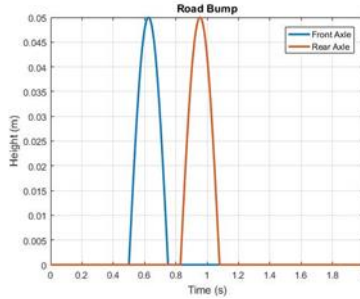


Figure 2 Road Bump based on sinusoidal function

3. OPTIMIZATION METHODS

In this paper, three optimization methods were examined. At first, Genetic (GA) and Gradient Based (GB) Algorithms were used in order to investigate their efficiency as well as to validate and understand their behaviour based on the theory of previous work [7 and 8]. Then, a hybridization of the above algorithms is tested in order to combine the advantages of each method and compare it with them.

Hybrid Algorithms form a new area of interest for the research community, and the optimization methods would not be the exception. Hybrid optimization algorithms combine two or more different optimization methods in order to solve a problem, switching between them over the course of the algorithm. In this way all the advantages of the involved methods are drafted in order to achieve the optimum result. For example, GA are more likely to find a global minimum, contrary to the GB which are often trapped, as well as the fact that the GA do not require the calculation of any derivative. Thus, the fitness function of the GA does not need to be continuous, so they are able to handle problems with discrete solution spaces. Furthermore, GB should be used when the area of the desired solution is known, in any other case the GA have better results due to their stochastic nature. Based on these points, a possible combination would be a stochastic method followed by a deterministic one. In the beginning, GA will operate for a number of generations with large population in order to locate the area of the optimum solution. After that, GB is employed so as to locate the global minimum, knowing the area of the desired solutions. The GA set of optimal values is used as initial value for the GB method, and the upper and lower bounds are set in a symmetric area around the initial values. Thus, the ability of GB methods to converge to a local (in this case global) minimum is exploited. The genetic part in the hybrid algorithm was active for 10 generations.

4. OPTIMIZATION PROCEDURE

The object of the optimization is the vehicle model, mentioned in chapter 1.1, and the target of the optimization is the optimum dynamic behaviour. The design variables selected are all the suspension parameters and specifically the vector below:

$$Design\ Variables = [K_{l_F}, K_{nl_F}, K_{l_R}, K_{nl_R}, C_F, C_R] \tag{8}$$

which are the linear and the nonlinear part of the spring as well as the damping coefficient of both the front and rear suspension system, see also Table 2.

Regarding the bounds of the design variables, the upper and lower ones were chosen based on experimental processes, previous works and the literature: They are

presented in Table 3. As far as the constraints are concerned, they were chosen in terms of the dynamic behaviour of the vehicle and the design of the suspension. Specifically, the root mean square of body's acceleration as well as the contribution of the non-linear term of the spring force were selected as the constraints of the optimization process being set under 1 (m/s²) and between 10-30% respectively.

Table 3 Lower and Upper Bounds of the Design Variables

Design Variables	Lower Bounds	Upper Bounds
K_{lF}, K_{lR} (N/m)	3.2·10 ⁴	1.5·10 ⁵
C_F, C_R (N/m·s)	2.0·10 ³	1.0·10 ⁴
K_{nlF}, K_{nlR} (N/m ³)	5·10 ⁵	3·10 ⁸

While regarding the fitness functions, it was decided to investigate single-objective problems in comparison with multi-objective ones. Thus, three single-objective problems were formulated regarding different targets of the dynamic behavior of the vehicle. The first target is the ride comfort of the driver and the safety of the truck load. This target is evaluated through the vehicle's body acceleration (*fitness*₁ - Case 1). The second one is the travel of both front and rear suspensions (*fitness*₂ - Case 2). The third one is the deflection of both front and rear tires, ensuring road holding (*fitness*₃ - Case 3). The mathematical equations of these targets were formed to the following three fitness functions (equation 9-11). In order to achieve better results, the variances (will be used as var (x)) of the values, which depict the optimization targets, were selected. Moreover, so as to include in the terms *fitness*₂ and *fitness*₃ both the values of the front and rear suspension travel and the values of front and rear tire deflection respectively, the average value of their variances was used. To conclude, three single objective problems were built with the following fitness and objective functions:

$$fitness_1 = var(acc_{body}) \quad (9)$$

$$fitness_2 = \frac{1}{2} \cdot [var(suspension.travel_F) + var(suspension.travel_R)] \quad (10)$$

$$fitness_3 = \frac{1}{2} \cdot [var(tire.deflection_F) + var(tire.deflection_R)] \quad (11)$$

Moreover, due to the fact that the three targets selected are in conflict, the optimal solution for each target would be different. Taking this conflict into consideration, the aforementioned targets were combined so as to formulate a multi-objective problem. In this way, it was possible to examine the balancing between the desired goals of the optimization and locate the optimum solution of the problem. In an attempt to save computational time, reduce the complexity of the problem and concentrate more to the comparison of the optimization methods, the multi-objective problem was converted into a single objective one through the sum of the three targets, mentioned in equations 9-11, as follows:

$$fitness = w_1 \cdot fitness_1 + w_2 \cdot fitness_2 + w_3 \cdot fitness_3 = f_1 + f_2 + f_3 \quad (12)$$

where w_1, w_2, w_3 are the weight factors. In order to investigate the multi-objective approach more accurately, two scenarios were tested. In the first scenario the magnitudes of

all the three terms (f_1, f_2 and f_3) were at the same order and balanced (*Case 4*). While in the second scenario with different weight factors, the term f_1 was selected as the main one and its magnitude was set one order greater than the ones of the two other terms, f_2 and f_3 (*Case 5*). The values of the weight factors were selected based on random simulations of the model.

The optimization was implemented with the Optimization Toolbox of MATLAB R2016a, provided for academic use by NTUA. The methods selected for the configured problem was a Genetic Algorithm (*ga of MATLAB*), a Gradient Based Algorithm (*active set of fmincon of MATLAB*) as well as a hybridization of the above. To sum up, 5 different scenarios (*S1-S5*), regarding the optimization methods, were implemented for 5 different cases as far as the fitness functions are concerned (*Case 1-5*). The set of the optimization scenarios is illustrated in Table 4 in detail. In S1 and S3, the population size was set to 200 as proposed in MATLAB R2016a for problems with more than 5 design variables (currently 6), whilst in S2 and S4, the population size was set to 1000 in order to investigate the influence of the population size. As far as the hybrid method is concerned, the part of the genetic algorithm was active only for 10 generations and then the gradient based algorithm was enabled.

Table 4 Implemented Optimization Scenarios for each Case

Implemented Optimization Scenarios for each Case					
Genetic Algorithm	S1	Population Size	200	Fitness Function Tolerance	10^{-6}
	S2	Population Size	1000		
Hybrid Algorithm	S3	Population Size	200	Fitness Function Tolerance	10^{-6}
	S4	Population Size	1000		
Gradient Based	S5	Objective Function Tolerance		10^{-6}	

5. RESULTS

The results will be presented for each case of fitness and objective function (*Case 1-5*). At first, in each case the optimal design variables will be presented for every optimization scenario (S1-S5). Furthermore, the RMS of the vehicle’s body acceleration, the maximum suspension travel of both front and rear suspensions and the maximum tire deflection through the front and rear tire forces, which are $K_{T_i}(x_i - y_i)$, will be illustrated after the simulation of the model for the optimal design variables.

5.1 Case 1

In this case, the fitness function was the variance of body’s acceleration. In terms of the objective function, the “best” optimal solution was found with optimization scenarios S4 and S5, which are the hybrid one with population 1000 and the gradient based algorithm respectively. In these scenarios, the fitness function, hence the term that depicts the ride comfort, reached to the minimum value, as it is shown both in Table 6, through the RMS of vehicle’s body acceleration, and in Figure 3, through the variance of vehicle’s body acceleration and term f_1 . Moreover, as far as the design variables are concerned, these two scenarios have converged to design variables closed to each other’s proving that the algorithms converged almost to the same solution. In addition, the contribution of the nonlinear part of the suspension spring is almost the same. In Table 5, the optimal solutions of the design variables verify the target of the optimization of this case, since in order to improve and secure the ride comfort, the optimization methods are trying to configure the

suspension system with low spring stiffness and low damping coefficient sacrificing the suspension travel. Finally, the computational time needed for the optimal solutions has to be mentioned due to the fact that the gradient based algorithm found the optimal solution in the 5% of the time that the hybrid algorithm converged.

Table 5 Optimal Solutions of Design Variables / Case 1

Design Variables	Optimization Scenarios				
	S1	S2	S3	S4	S5
K_{lF} (N/m)	102620	34479	105019	43094	36194
C_F (N·s/m)	6950	2000	5890	2050	2582
K_{lR} (N/m)	32352	74939	58027	33652	39741
C_R (N·s/m)	2083	5112	2155	2272	3228
K_{nlF} (N/m ³)	1.97*10 ⁷	3.42*10 ⁶	4.08*10 ⁷	1.09*10 ⁷	1.03*10 ⁷
K_{nlR} (N/m ³)	8.58*10 ⁶	4.47*10 ⁷	1.30*10 ⁷	9.19*10 ⁶	1.18*10 ⁷

Table 6 Vehicle Model's Parameters for the Optimal Solutions / Case 1

Vehicle Model's Parameters	Optimization Scenarios				
	S1	S2	S3	S4	S5
RMS(accbody) (m/s ²)	0.631	0.561	0.682	0.450	0.470
Max. Suspension Travel Front (m)	0.025	0.037	0.024	0.040	0.037
Max. Suspension Travel Rear (m)	0.038	0.027	0.038	0.038	0.037
Max. Tire Force Front (N)	4085	2249	3833	2991	2649
Max. Tire Force Rear (N)	3061	3750	3275	2610	2791
Nonlinear% of Front Spring Force	11	12	19	29	28
Nonlinear% of Rear Spring Force	27	30	24	29	28

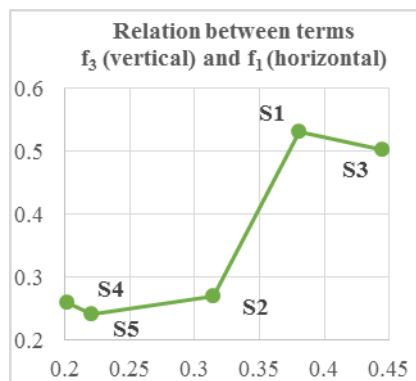
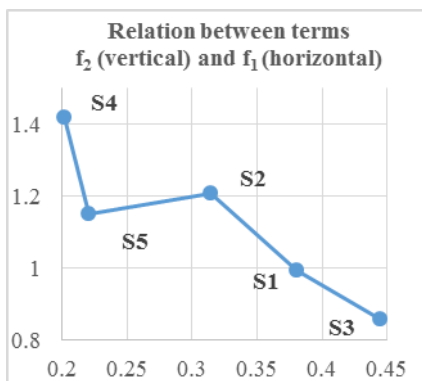


Figure 3 Relation between terms (a) f₂ and f₁ (b) f₃ and f₁ / Case 1

5.3 Case 2

In this case, the fitness function was the average of the variances of both front and rear suspension travels. In terms of the objective function, the “best” optimal solution was found with optimization scenarios S2, S3 and S4 which are the genetic algorithm with population 1000 and the hybrid ones with population 200 and 1000, respectively. In these scenarios, the fitness function, hence the term that depicts the suspension travel, reached to the minimum value of all the scenarios as it is shown both in Table 8, through the maximum value of both the front and rear suspension travels, and in Figure 4, through the average of the variances of the front and rear suspension travels, hence term f2. Moreover, as far as the design variables are concerned, the two scenarios, S2 and S4, have reached to close values proving that the algorithms converged to almost the same optimal solution.

Table 7 Optimal Solutions of Design Variables / Case 2

Design Variables	Optimization Scenarios				
	S1	S2	S3	S4	S5
$K_{IF}(N/m)$	83283	51337	38952	57879	51377
$C_F(N\cdot s/m)$	6635	9696	8003	8759	2003
$K_{IR}(N/m)$	70210	36651	47540	36934	36456
$C_R(N\cdot s/m)$	9091	8757	8286	9376	2001
$K_{nlF}(N/m^3)$	$2.57\cdot 10^7$	$2.48\cdot 10^7$	$2.56\cdot 10^7$	$1.30\cdot 10^7$	$7.56\cdot 10^7$
$K_{nlR}(N/m^3)$	$3.42\cdot 10^7$	$1.37\cdot 10^7$	$1.60\cdot 10^7$	$1.84\cdot 10^7$	$2.96\cdot 10^7$

On the other hand, the optimization scenario S3 differs mainly on the linear part of the spring both to the front and the rear suspensions, proving that has selected a solution with different characteristics which could also be shown by its lower value of the RMS of the vehicle’s body acceleration. In Table 7, the optimal design variables of the current case verify the target of the optimization, due to the configuration of both higher spring stiffness and damping coefficient in order to secure the minimum suspension travel in contrary to the previous case. In addition, the failure of the gradient based algorithm has to be mentioned, due to the lack of compability between both the design variables in Table 7 and the vehicle parameters in Table 8 with the objective of the optimization, which is the minimization of the suspension travel.

Table 8 Vehicle Model’s Parameters for the Optimal Solutions / Case 2

Vehicle Model’s Parameters	Optimization Scenarios				
	S1	S2	S3	S4	S5
RMS(accbody) (m/s^2)	0.989	0.994	0.908	0.980	0.470
Max. Suspension Travel Front (m)	0.030	0.025	0.026	0.026	0.041
Max. Suspension Travel Rear (m)	0.020	0.021	0.022	0.021	0.038
Max. Tire Force Front (N)	4682	4168	3571	3957	3212
Max. Tire Force Rear (N)	3559	3276	3384	3364	3462

Nonlinear % of Front Spring Force	22	23	30	13	20
Nonlinear % of Rear Spring Force	16	15	14	18	10

Finally, the computational time needed for the optimal solutions for optimization scenario S4 has dropped to the 50% of the time needed in S2, proving the importance of the hybrid algorithm and its effectiveness, as in both scenarios the optimal solution are similar. Additionally, in S3 due to the lower population and the hybrid algorithm, the problem converged to almost the 10% of the time in comparison with S2.

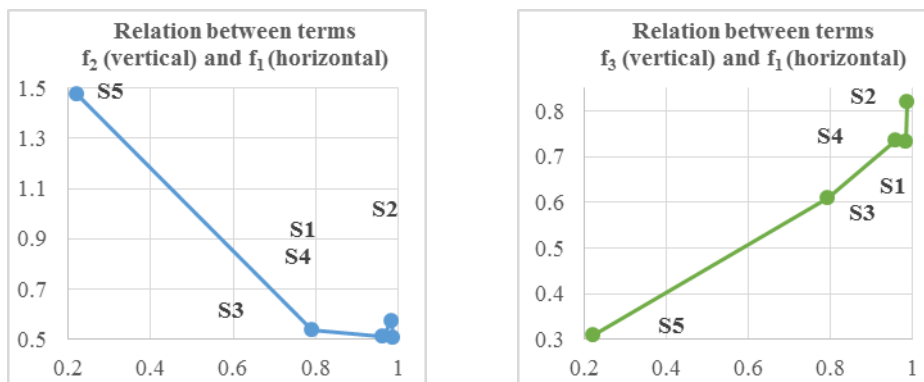


Figure 4 Relation between terms (a) f_2 and f_1 (b) f_3 and f_1 / Case 2

5.3 Case 3

In this case, the fitness function was the average of the variances of both front and rear tire deflections. In terms of the objective function, the “best” optimal solution was found by the optimization scenarios S2 and S3 which are the genetic algorithm with population 1000 and the hybrid one with population 200. In these scenarios, the fitness function, hence the term that depicts the tire deflection, reached to the minimum value of all the scenarios as it is shown both in Table 10, through the maximum value of both the front and rear tire forces, and in Figure 5, through the average of the variances of the front and rear tire deflections, hence term f_3 . Moreover, as far as the design variables are concerned, the two scenarios, S2 and S3, have reached to close values proving that the algorithms found almost the same optimal solution. The only difference between the design variables in these two scenarios is the contribution of the nonlinear part of the spring of both front and rear suspensions. Despite the different population used in this two scenarios (S2 and S3), the hybrid algorithm with the lower population (S3) has succeeded in comparison with the genetic algorithm with the greater population (S2). The hybrid algorithm overcame the disadvantage of the lower population combining the advantages of both the genetic and the gradient based algorithm, leading to the optimal solution in a computational time of almost 8% of the time of optimization scenario S2. The success is confirmed due to the close solutions of the design variables as well as the values of the important parameters of the vehicle’s model. Finally, the effectiveness of the gradient based algorithm, in this current case, is based on the connection of the tire deflection and the RMS of vehicle’s body acceleration, which is illustrated in Figures 3b-5b of all the cases. Particularly, the increase or the decrease of the term f_1 , which depicts the ride comfort, leads to the increase or the decrease of term f_3 , which depicts the tire deflection, respectively.

Table 9 Optimal Solutions of Design Variables / Case 3

Design Variables	Optimization Scenarios				
	S1	S2	S3	S4	S5
K_{IF} (N/m)	41279	33114	37028	47186	33583
C_F (N·s/m)	3632	2139	2092	2203	4242
K_{IR} (N/m)	77718	65367	67512	57595	37473
C_R (N·s/m)	4319	3661	4211	2713	2000
K_{nlF} (N/m ³)	1.44*10 ⁷	4.95*10 ⁶	1.11*10 ⁷	8.54*10 ⁶	1.23*10 ⁷
K_{nlR} (N/m ³)	5.00*10 ⁷	2.69*10 ⁷	3.47*10 ⁷	2.62*10 ⁷	3.31*10 ⁶

Table 10 Vehicle Model's Parameters for the Optimal Solutions / Case 3

Vehicle Model's Parameters	Optimization Scenarios				
	S1	S2	S3	S4	S5
RMS(accbody) (m/s ²)	0.637	0.520	0.556	0.529	0.466
Max. Suspension Travel Front (m)	0.033	0.036	0.037	0.038	0.031
Max. Suspension Travel Rear (m)	0.025	0.032	0.029	0.031	0.040
Max. Tire Force Front (N)	2936	2226	2515	2853	2596
Max. Tire Force Rear (N)	3381	3537	3569	3006	3111
Nonlinear % of Front Spring Force	27	16	30	21	26
Nonlinear % of Rear Spring Force	29	29	30	30	12

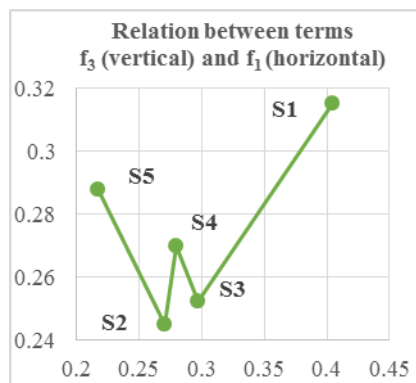
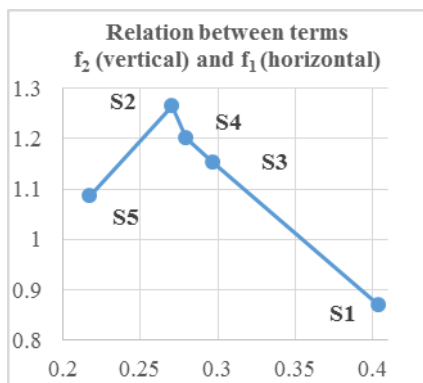


Figure 5 Relation between terms (a) f₂ and f₁ (b) f₃ and f₁ / Case 3

5.4 Case 4

In this case, the fitness function was the sum of all the three terms (f₁, f₂ and f₃) which were at the same order and balanced. First of all, as far as the effectiveness of the

algorithms is concerned, the gradient based wasn't able to find a "good" optimal solution, getting trapped probably in a local minimum. This conclusion is verified by the fact that all the design variables reached the lower bounds without giving a proper solution, while the optimization process ended in only 43 seconds. Due to the multi-objective character of this case it's difficult to understand which optimization scenarios converged to the "best" optimal solutions. On the other hand, the differences in the optimal design variables in every optimization scenario have to be mentioned. In contrary with the previous cases, none of the optimal design variables are close enough to indicate the same characteristics of the solutions, but Table 12, based on the values of important parameters of the vehicle model, points out some common characteristics between optimization scenarios of S2-S4, such as the maximum suspension travels and the maximum tire forces indicating probably common characteristics to the solutions.

Table 11 Optimal Solutions of Design Variables / Case 4

Design Variables	Optimization Scenarios				
	S1	S2	S3	S4	S5
K_{IF} (N/m)	81307	46116	63116	42377	32000
C_F (N·s/m)	5431	4129	3645	4002	2000
K_{IR} (N/m)	57264	45371	66731	60069	32000
C_R (N·s/m)	2877	5301	2753	3693	2000
K_{nIF} (N/m ³)	$2.12 \cdot 10^7$	$6.24 \cdot 10^6$	$1.78 \cdot 10^7$	$1.36 \cdot 10^7$	$5.00 \cdot 10^6$
K_{nIR} (N/m ³)	$9.52 \cdot 10^6$	$2.73 \cdot 10^7$	$3.47 \cdot 10^7$	$2.86 \cdot 10^7$	$1.08 \cdot 10^7$

Table 12 Vehicle Model's Parameters for the Optimal Solutions / Case 4

Vehicle Model's Parameters	Optimization Scenarios				
	S1	S2	S3	S4	S5
RMS(accbody) (m/s ²)	0.666	0.611	0.635	0.589	0.370
Max. Suspension Travel Front (m)	0.028	0.033	0.031	0.031	0.039
Max. Suspension Travel Rear (m)	0.033	0.027	0.028	0.029	0.048
Max. Tire Force Front (N)	3704	3096	3270	2802	2103
Max. Tire Force Rear (N)	2805	2785	2937	3105	3086
Nonlinear % of Front Spring Force	17	13	21	24	12
Nonlinear % of Rear Spring Force	15	30	29	29	17

5.5 Case 5

In this case, the fitness function was the sum of all the three terms (f_1 , f_2 and f_3) where the main term was f_1 and the other two were set one order of magnitude lower. The main idea in this case was the use of the two targets more as penalties rather than targets of the optimization; this is the reason why f_2 and f_3 were one order of magnitude lower. First of all, regarding the effectiveness of the algorithms, the gradient based seems to concentrate to optimize only the term f_1 , which depicts the ride comfort, ignoring the multi-objective

character of this fitness function and failing to find a “good” optimal solution. This problem is also pointed out in the design variables of this optimization scenario (S5) in which some of them are trapped in the upper or lower bounds, as well as the time the problem needed to converge. The results of this case, regarding the gradient based algorithm, prove the conclusions indicated above regarding the effectiveness of the algorithm. As far as the other optimization scenarios are concerned, due to the multi-objective character of this case it is difficult to understand which optimization scenarios converged to the “best” optimal solutions. Moreover, in contrary with the previous case, neither the optimal design variables in every optimization scenario nor the table of the important parameters of vehicle’s model could indicate similar characteristics in the optimal solutions.

Table 13 Optimal Solutions of Design Variables / Case 5

Design Variables	Optimization Scenarios				
	S1	S2	S3	S4	S5
$K_{IF}(N/m)$	59559	49457	43581	37635	44761
$C_F(N\cdot s/m)$	2414	2164	5312	2096	2000
$K_{IR}(N/m)$	58680	56541	45694	65343	45798
$C_R(N\cdot s/m)$	3901	6281	1910	4616	2000
$K_{nIF}(N/m^3)$	$1.25\cdot 10^7$	$5.72\cdot 10^6$	$2.42\cdot 10^7$	$5.09\cdot 10^6$	$7.56\cdot 10^6$
$K_{nIR}(N/m^3)$	$4.34\cdot 10^7$	$4.40\cdot 10^7$	$5.89\cdot 10^6$	$3.32\cdot 10^7$	$3.56\cdot 10^6$

Table 14 Vehicle Model’s Parameters for the Optimal Solutions / Case 5

Vehicle Model’s Parameters	Optimization Scenarios				
	S1	S2	S3	S4	S5
RMS(acc_{body}) (m/s^2)	0.605	0.587	0.538	0.538	0.466
Max. Suspension Travel Front (m)	0.038	0.040	0.026	0.038	0.040
Max. Suspension Travel Rear (m)	0.024	0.023	0.036	0.029	0.038
Max. Tire Force Front (N)	3556	3070	2829	2433	2836
Max. Tire Force Rear (N)	2549	2944	3154	3367	3302
Nonlinear % of Front Spring Force	23	16	27	16	21
Nonlinear % of Rear Spring Force	30	30	14	30	10

6. DISCUSSION

In order to compare all the optimal solutions retrieved with all the optimization Scenarios and all Cases, the optimal design points retrieved with Cases 1 - 3 and 5 were scaled to Case 4. Case 4 was selected as the ground Case due to its multi - objective character. In more details, the vehicle model was simulated with each set of the optimal design variables and the terms f_1 , f_2 and f_3 have been recalculated and hence the optimal value of the fitnesses based on Case 4, leading to the comparison presented in Figure 6 and Table 15. In Figure 6, the fitness’ value of each optimization scenario (S1-S5 (different group of columns)) is compared for all the cases (Case 1-5 (columns of different color)). In

the Table of data of the figure, the optimum solution for every Case is pointed out in borders of the corresponding color. The comparison of the fitness' values is performed horizontally. In addition, Table 15 presents the values of the terms f_1, f_2 and f_3 as well as the sum of them for the optimum solution for each case, in addition with the optimization scenario in which it was found. The sum of the terms is the fitness values of the optimal solutions scaled to Case 4 and also presented in the data table of Figure 6.

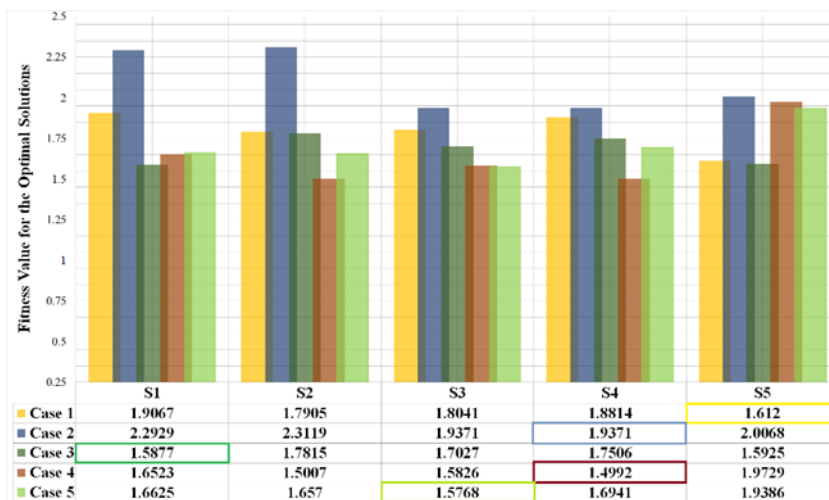


Figure 6 Comparison of the Optimal Solutions based on the values of Optimal Fitnesses

Table 15 Comparison of the Fitness Values of the Optimal Solutions

Terms	Case 1	Case 2	Case 3	Case 4	Case 5
	S5	S4	S1	S4	S3
f_1	0.221	0.7921	0.4042	0.3466	0.2758
f_2	1.15	0.536	0.8685	0.8532	0.963
f_3	0.241	0.609	0.315	0.2994	0.338
$f_1+f_2+f_3$	1.612	1.9371	1.5877	1.4992	1.5768

Table 16 Comparison of the Design Variables of the Optimal Solutions

Design Variables	Case 1	Case 2	Case 3	Case 4	Case 5
	S5	S4	S1	S4	S3
K_{lF} (N/m)	36194	38952	41279	42377	43581
C_F (N·s/m)	2582	8003	3632	4002	5312
K_{lR} (N/m)	39741	47540	77718	60069	45694
C_R (N·s/m)	3228	8286	4319	3693	1910

K_{nlF} (N/m ³)	1.03*10 ⁷	2.56*10 ⁷	1.44*10 ⁷	1.36*10 ⁷	2.42*10 ⁷
K_{nlR} (N/m ³)	1.18*10 ⁷	1.60*10 ⁷	5.00*10 ⁷	2.86*10 ⁷	5.89*10 ⁶

At first, regarding the optimum solution of all the results, based on Table 15 and Figure 6, could be found in Case 4/S4 which was expected because Case 4 was the ground case for comparison of the optimal solutions. The next two near the optimum solution, were the one of Case 5/S3 as well as the one of Case 3/S1. Based on Table 15, the close values of the terms f_1 , f_2 and f_3 of Case 4/S4 and Case 3/S1 show that they have converged to almost the same solution in combination with the optimal design variables of these solutions, as shown in Table 16. The only difference in the design variables of these two solutions is the stiffness of the rear suspension system which lead to the slightly higher term f_1 , which depicts the ride comfort, in Case 3/S1 (0.4042) than Case 4/S4 (0.3466). On the other hand, Case 5/S3 appears to have converged to a different family of solutions. More specifically, in Case 5/S3 the rear suspension system is configured to lower values of the stiffness of the spring and of the damping coefficient than the optimal solutions of the other cases, as shown in Table 15, improving the ride comfort by decreasing term f_1 and increasing term f_2 , representing the ride comfort and the suspension travel respectively, as shown in Table 16. Furthermore, Case 5/S3 achieved a solution better than this of the single objective of term f_1 (Case 1/S5), but slightly worse than the multi-objective with f_1 , f_2 and f_3 balanced (Case 4/S4). This suggests that using the terms f_2 and f_3 as penalties, the optimization prioritizes the main term taking slightly into consideration the other two, leading to a middle ground solution. This is why the optimum solution of Case 5 is a combination of the characteristics of Case 1/S5 and Case 4/S4.

Regarding the optimization scenarios, the Hybrid Algorithm was the leading method either with population 200 (S3) or 1000 (S4), outnumbering the other methods, as shown in Table 15, where the three of the five optimal solutions are found through hybrid algorithms. Secondly, the gradient based algorithm proved its reliability in Case 1 and Case 3 in contrary to the other cases in which it failed. Based on the discussion in Cases 1-3, the gradient based algorithm (S5) could deliver acceptable results only when the RMS of vehicle's body acceleration is connected directly and straight forward with the target of the optimization. This is the reason of its effectiveness in Case 3, where the fitness function, which depicts the average of both the front and rear tire deflections (f_3), increases or decreases according to the increase or the decrease of the RMS of vehicle's body acceleration, which depicts the ride comfort (f_1), as shown in Figures 3b-5b.

As far as the different Cases are concerned, based on the data table of Figure 6, Case 3 seems to be superior than Case 1 due to the fact that the optimal values of the fitnesses in the line of Case 3 are always lower than the ones of Case 1, regardless the optimization scenarios. Moreover, in all the optimization scenarios, Case 3 not only delivered more satisfactory optimal solutions than Case 1 but also converged in much less computational time, lowering it by 10-40% depending on the optimization scenario. The argument regarding the superiority of Case 3, is validated from the fact that it delivered one of the most satisfactory optimal solution in comparison with the results of Case 4, as explained in the previous paragraphs in detail. Combining the above points, Case 3 converge to solutions taking into consideration not only the increase of the ride comfort but also the minimization of the suspension travel, indicating a multi-objective character despite having a single-objective fitness function. Moreover, based on Figure 6, Case 3 seems to be stable in providing satisfactory optimal results in comparison with all the other cases which sometimes fail to deliver depending the optimization scenario.

6. CONCLUSIONS

To sum up, in the current paper the optimization of a heavy vehicle's suspension system were investigated setting different optimization targets. Conclusions have been made not only regarding the fitness functions but also for the optimization methods used in order to reach the optimum solution more accurately and with less computational time. The remarks regarding Case 3, discussed in the previous section, outline the importance of tire deflection being a part of the fitness function due to the superiority of Case 3 over Case 1. Due to its multi-objective character, Case 3 seems to outnumber Case 1, which is the most common main term of fitness functions in literature as far as the optimization of suspension systems is concerned. This could lead to the use of the tire deflection, as the main target in the optimization of suspension systems in combination with various existing methods of the literature mentioned in the introduction. Furthermore, the effectiveness of the hybrid algorithm proved promising in comparison with the other algorithms. They were able to find more satisfactory solutions in most cases and with less computational time than the other algorithms. The most important regarding the hybrid algorithms is the need of finding the balance between the use of its genetic and gradient based parts so as to gain more from the hybridization and help the problem to converge in less time. Further work is in progress to extend our research.

REFERENCES

- [1] Georgiou, G., Verros, G., & Natsiavas, S. (2007), "Multi-objective optimization of quarter-car models with a passive or semi-active suspension system", *Vehicle System Dynamics*, 45(1), pp 77-92.
- [2] Özcan, D., Sönmez, Ü., & Güvenç, L. (2013), "Optimization of the nonlinear suspension characteristics of a light commercial vehicle", *International Journal of Vehicular Technology*, 2013.
- [3] Shirahatti, A., Prasad, P. S. S., Panzade, P., & Kulkarni, M. M. (2008), "Optimal design of passenger car suspension for ride and road holding", *Journal of the Brazilian Society of Mechanical Sciences and Engineering*, 30(1), 66-76.
- [4] Gündoğdu, Ö. (2007), "Optimal seat and suspension design for a quarter car with driver model using genetic algorithms", *International Journal of Industrial Ergonomics*, 37(4), 327-332.
- [5] Alkhatib, R., Jazar, G. N., & Golnaraghi, M. F. (2004), "Optimal design of passive linear suspension using genetic algorithm", *Journal of Sound and vibration*, 275(3), pp 665-691.
- [6] D. Koulocheris, H. Vrazopoulos and V. Detrimanis (2002), "Optimization Algorithms for tuning suspension systems used in ground vehicles", *Proceeding of International Body Engineering Conference & Exhibition and Automotive & Transportation Technology Conference*, Paris, France, July 2002, SAE Paper no. 2002-01-2214.
- [7] Koulocheris D., Papaioannou G., Christodoulou D. (2016), "Multi objective optimization of a heavy vehicle nonlinear suspension system", *Proceedings of the 11th International Congress of Mechanics (11th HSTAM)*, Athens, Greece, 27-30 May 2016.
- [8] Koulocheris D., Papaioannou G. (2016), "Experimental evaluation of the vertical wheel loads of a heavy vehicle validated with an optimized half car model", *Proceedings of the 11th International Congress of Mechanics (11th HSTAM)*, Athens, Greece, 27-30 May 2016.

- [9] Koulocheris D., Papaioannou G. (2015), "Dynamic Analysis of the Suspension System of a Heavy Vehicle through Experimental and Simulation Procedure", Proceedings of 25th International Automotive Conference "Science and Motor Vehicles" (25th JUMV), Beograd, Serbia, 14-15 April 2015.
- [10] Sun, L., Cai, X., & Yang, J. (2007), "Genetic algorithm-based optimum vehicle suspension design using minimum dynamic pavement load as a design criterion", *Journal of Sound and Vibration*, 301(1), 18-27.
- [11] Uys, P. E., Els, P. S., & Thoresson, M. (2007), "Suspension settings for optimal ride comfort of off-road vehicles travelling on roads with different roughness and speeds", *Journal of Terramechanics*, 44(2), pp 163-175.

Intentionally blank

HYDRODYNAMIC EFFECTS IN COMMON RAIL FUEL SYSTEM IN CASE OF MULTIPLE INJECTION OF DIFFERENT FUELS

Mikhail G. Shatrov , Leonid N. Golubkov, Andrey U. Dunin, Pavel V. Dushkin, Andrey L. Yakovenko¹

UDC:621.436.038

ABSTRACT: Fuel injection by Common Rail type fuel system results in hydrodynamic effects presenting considerable interest in case of multiple injections. After injection, fuel pressure oscillations at the injector inlet originate which influence considerably the injection rate and characteristic of consequent injection in case of multiple injections. The article presents the results of various factors influence experimental research on pressure oscillations at the injector inlet in case of single and doubles injections of different fuels. With this, such factors as fuel pressure, injection rate value, interval between injections, physical properties of fuel and design features of the injector were taken into account. The aim of the research: to evaluate the influence of pressure oscillations caused by the preliminary injection of fuel to the main injection. Analysis of the experimental data obtained is useful for selection of main design solutions for Common Rail Injectors (CRI).

KEY WORDS: common rail type fuel system, common rail injector, hydrodynamic effects, pressure oscillations, fuel injection rate

HIDRODINAMIČKI EFEKTI KOD COMMON RAIL SISTEMA UBRIZGAVANJA GORIVA SA VIŠE BRIZGAČA RAZLIČITIH GORIVA

REZIME: Ubrizgavanje goriva kod Common Rail sistema izaziva hidrodinamičke efekte koji predstavljaju značajan interes kada postoji više brizgača u sistemu. U slučaju kada postoji više brizgača, nakon ubrizgavanja, oscilacije pritiska goriva na ulazu znatno utiču na brzinu i karakteristike ubrizgavanja. U radu su predstavljeni rezultati uticaja različitih faktora eksperimentalnih istraživanja oscilacija pritiska na ulazu brizgača u slučaju jednog i dva brizgača različitih goriva. Parapmetri: pritisak goriva, brzina brizganja, interval između ubrizgavanja, fizičke osobine goriva i karakteristike brizgača uzeti su u obzir. Cilj istraživanja je bio proceniti uticaj oscilacija pritiska izazvanih prethodnim ubrizgivanjem goriva do glavnog brizgača. Analiza dobijenih eksperimentalnih podataka je korisna za izbor rešenja brizgača koji se koristi u Common Rail sistemu.

KLJUČNE REČI: common rail sistem ubrizgavanja goriva, common rail brizgač, hidrodinamički efekti, oscilacije pritiska, brzina ubrizgavanja goriva

¹ Received: September 2016, Accepted October 2016, Available on line November 2016

HYDRODYNAMIC EFFECTS IN COMMON RAIL FUEL SYSTEM IN CASE OF MULTIPLE INJECTION OF DIFFERENT FUELS

*Mikhail G. Shatrov*¹, *Leonid N. Golubkov*², *Andrey U. Dunin*³, *Pavel V. Dushkin*⁴, *Andrey L. Yakovenko*⁵

UDC: 621.436.038

1. INTRODUCTION

Accumulator type fuel systems (Common Rail) are widespread due to their capability of in a timely manner depending on the mode of operation of the diesel engine to arrange the high pressure multiple injection with high precision.

As fuel systems are improved, the maximal injection pressure grows [8, 10]. In a number of publications, the issue of the need of injecting fuel under the pressure over 2500 bar is discussed [5, 6, 7, 9].

The pressure growth in case of multiple injection makes the fuel injection working process more complicated. Pressure oscillations at the injector inlet become more crucial which was noted by many researchers [1, 2, 3] including in MADI.

Applied research and experimental developments are carried out with financial support of the state represented by the Ministry of Education and Science of the Russian Federation under the Agreement No 14.580.21.0002 of 27.07.2015, the Unique Identifier PNIER: RFMEFI58015X0002.

2. EXPERIMENTAL SETUP

2.1 Measuring equipment

For carrying up experimental research of Common Rail diesel engine fuel systems, at the Department of Heat Engineering and Automobile and Tractor Engines of MADI, an experimental setup was developed on the base of a bench with low pressure fuel line and electric drive of a high pressure (HP) fuel pump. Common Rail fuel systems of various configurations may be mounted on the bench depending on the kind of the problem being handled.

For carrying out investigations, the station was complemented with measuring system having two piezoelectric sensors. The first sensor is mounted at the inlet of the common rail injector (CRI) and registers the pressure oscillations when fuel is injected. The second sensor is mounted in the chamber and registers the instants of fuel injection start and

¹ *Mikhail G. Shatrov, professor, University of MADI, Leningradsky Prosp.,64, Moscow, 125319, Russia, dvs@madi.ru*

² *Leonid N. Golubkov, professor, University of MADI, Leningradsky Prosp.,64, Moscow, 125319, Russia, dvsgolubkov@yandex.ru*

³ *Andrey U. Dunin, assist. prof., University of MADI, Leningradsky Prosp.,64, Moscow, 125319, Russia, a.u.dunin@yandex.ru*

⁴ *Pavel V. Dushkin, post-graduate student, University of MADI, Leningradsky Prosp.,64, Moscow, 125319, Russia, levvap@gmail.com*

⁵ *Andrey L. Yakovenko, assist. prof., University of MADI, Leningradsky Prosp.,64, Moscow, 125319, Russia, yakovenko_home@mail.ru*

end. The chamber presents an enclosed volume with a pressure discharge valve. The measuring system components are presented in Table 1.

Electronic control of fuel system is effected with the aid of microprocessor control system developed in MAD1. Measurement of injection rates was carried out using Collection of fuel for measuring injection rates is carried out with laboratory graduated jars.

Table 1 Measuring equipment

Name	Tool description
AVL A03 (Austria)	Dual-channel charge amplifier.
T6000 No 4636 (Russia)	Piezoelectric sensor. Sensibility: 2.1 pC/bar. Pressure measuring range 0...6000 bar.
T6000 No 4588 (Russia)	Piezoelectric sensor. Sensibility: 2.2 pC/bar. Pressure measuring range 0...6000 bar.
DMP304 (Germany)	Strain-gage sensor. Pressure measuring range 0...4000 bar.
Siglent AKIP 4126/2 (China)	Digital storage oscilloscope.

2.2 Configuration of fuel system and injection control

The fuel system includes: radial-plunger type HP fuel pump with throttle valve for fuel entering the pump, fuel accumulator with pressure sensor and two electro-hydraulic injectors. Parameters of its elements are presented in Table 2.

Table 2 Basic parameters of fuel system elements

Fuel system element	Parameters
CRI No1	No integrated fuel accumulator, pressure unbalanced valve, fuel injector nozzle hole diameter $d_c=0.12$ mm, number of holes 7.
CRI No2	Integrated fuel accumulator is present, pressure balanced valve, fuel injector nozzle hole diameter $d_c=0.09$ mm, number of holes 8.
Fuel line	Fuel line length $l_{\eta}=1000$ mm, channel diameter $d_{\eta}=2.2$ mm.

In both injectors, electromagnetic drive of the control valve is used. The second injector differs from the first one with the presence of a fuel accumulator integrated into the body and the design of the pressure balanced valve. Layouts of the injectors are presented in Figure 1.

The experiment was carried out in two stages: the first stage – the injector operate in case of a single injection; the second stage – the injector operate in case of multiple injection.

3. SINGLE INJECTION

At the first stage, the influence of the following factors on pressure oscillations at the CRI inlet was investigated (Figure 2): fuel pressure p_{ac} , control impulse duration τ_{imp} , type of fuel used. With this, two different injectors having principally different design were estimated in the experiment.

Fuel injection causes considerable oscillations of fuel pressure at the injector inlet. One of the reasons is hydraulic impact originating when closing the injector nozzle needle. In this way, in the injector No1 with pressure $p_{ac}=1000$ bar and control impulse duration $\tau_{imp}=0.6$ ms (corresponds to injection rate $Q=16.5$ mg), the injection causes pressure oscillations with amplitude up to 250 bar (Figure 3). Evidently, these oscillations influence the fuel supply process in case of multiple injections: the previous injections would influence on the following ones.

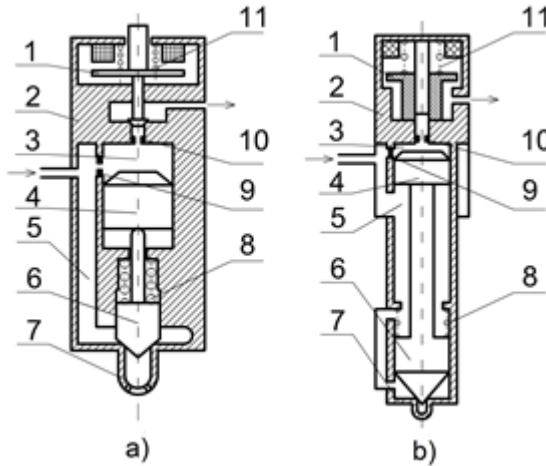


Figure 1 Layouts of the injectors:
a – injector No1, b – injector No2;

1 – control valve; 2 – CRI body; 3 – control chamber; 4 – multiplier (for version b, elements 4 and 6 are one piece); 5 (a) – channel supplying fuel to the injector nozzle; 5 (b) – fuel accumulator; 6 – injector nozzle needle; 7 – injector nozzle

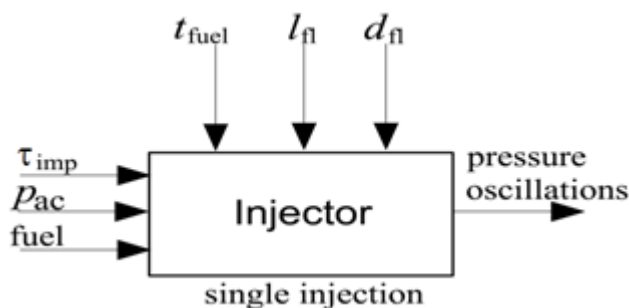


Figure 2 Layout of the first stage of the experiment:
controlled factors: τ_{imp} – control impulse duration, p_{ac} – pressure in the fuel accumulator, $fuel$ – working fluid (diesel fuel or sunflower oil); uncontrolled factors: t_{fuel} – fuel temperature, l_{fl} – fuel line length, d_{fl} – fuel line diameter

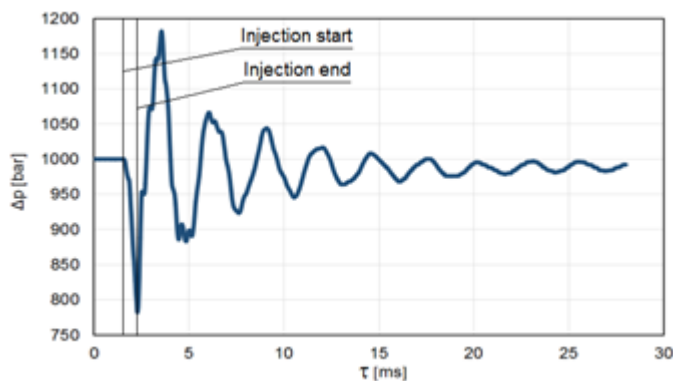


Figure 3 Pressure at the inlet of the CRI No 1 ($p_{ac}=1000$ bar, $\tau_{imp}=0.6$ ms)

As the fuel pressure and injection rate increase, the oscillation process increases. Figure 4 shows the comparison of data at three pressures in the fuel accumulator and constant control impulse duration $\tau_{imp}=0.6$ ms. A single injection is used. The pressure oscillation range at the CRI inlet at $p_{ac}=1500$ bar is up to 350 bar, and at $p_{ac}=500$ bar, the amplitude decreases to 80 bar.

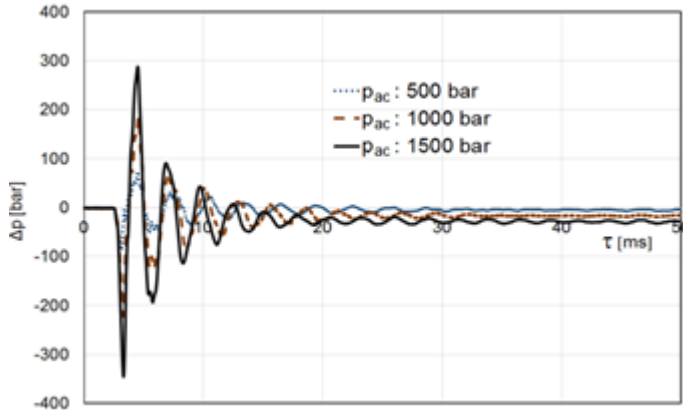


Figure 4 Fuel pressure oscillations at the entry of the CRI No1 at various pressures ($\tau_{imp}=0.6$ ms)

Figure 5 shows the comparison at constant pressure in the fuel accumulator $p_{ac}=1000$ bar and variation of the first control impulse duration. On the basis of this, one can make a conclusion that as the first portion of fuel decreases, the oscillations range also decreases.

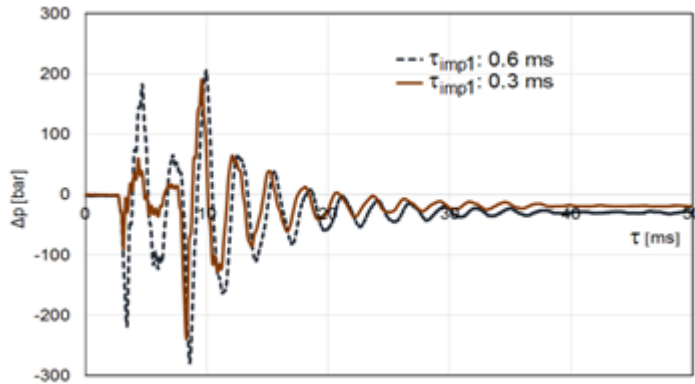


Figure 5 Fuel pressure oscillations at the entry of the CRI No1 at various duration of the first injection ($p_{ac}=1000$ bar)

Figure 6 shows the data for the injector No2 at the operation mode $p_{ac}=1000$ bar and $\tau_{imp}=0.6$ ms. Compared with the No1 version of the CRI (Figure 3), the pressure oscillations are considerably lower. The pressure oscillations range for the version No1 is 400 bar, and for the version No2 – 120 bar, that is, 3.3 times lower. Hence, the internal volume of the injector plays a considerable role and may be an efficient measure for lowering pressure oscillations.

The injector No2, has a pressure balanced valve in addition to integrated fuel accumulator. The balanced valve makes it possible not only to decrease the volume of fuel leaks at high pressure, but also to improve the injector working process in case of multiple injection [4].

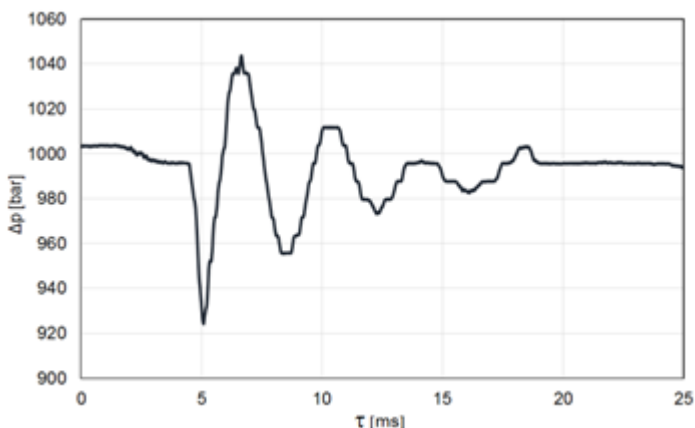


Figure 6 Pressure at the inlet of the CRI No2 ($p_{ac}=1000$ bar, $\tau_{imp}=0.6$ ms)

Physical properties of fuel used are also important in case of fuel injection. As the viscosity of fuel increases, the hydraulic friction grows which contributes to rapid damping of oscillations. Figure 7 shows the data for the injector No1 when operating on sunflower oil. As compared with diesel fuel (Figure 3), the oscillations range decreases from 400 bar to 250 bar at the same operating mode.

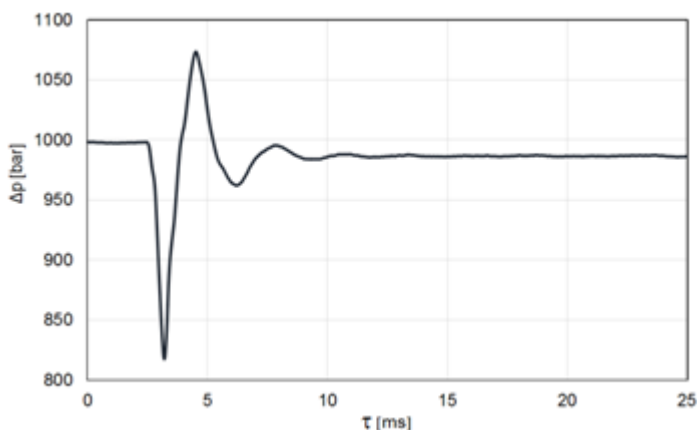


Figure 7 Pressure at the inlet of the CRI No1 ($p_{ac}=1000$ bar, $\tau_{imp}=0.6$ ms),
operation on sunflower oil

4. HYDRODYNAMIC EFFECTS IN CASE OF MULTIPLE INJECTION

At the second stage, the influence of the interval between the impulses of a double injection on the injection rate value of the second portion was investigated. In this experiment, the injector No1 was used. The layout of the second stage of the experiment in case of a double injection is presented in Figure 8.

The oscillogram of a current passing through electric magnet of injector No1 is shown in Figure 9. The injector control is carried out in two phases: forcing and holding. For forcing, voltage of about 50 V is applied to the electric magnet during 0.3 ms which promotes a rapid raise of the control valve. The injector needle is held using pulse-width modulation with duty ratio 50%.

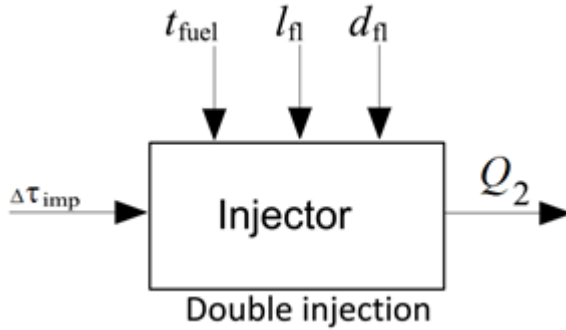


Figure 8 Layout of the second stage of the experiment:
 controlled factor: $\Delta\tau_{imp}$ – interval between two portions of a double injection; uncontrolled factors: t_{fuel} – fuel temperature, l_{fl} – fuel line length, d_{fl} – fuel line diameter; output parameter: Q_2 – injection rate of the second portion of a double injection

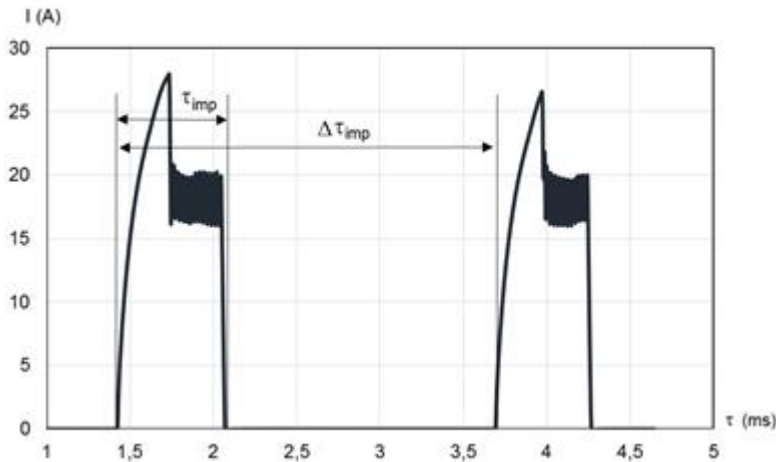


Figure 9 Oscillogram of current passing through electric magnet of injector No1 (double injection): τ_{imp} – control impulse duration, $\Delta\tau_{imp}$ – interval between two portions of double injection

Injector rate and injection characteristic of the second portion depend on the time at which the second injection is effected related to the first one. Figure 10 shows the results of the investigations at constant pressure $p_{ac}=1000$ bar, two injections each having $\tau_{imp}=0.6$ ms with variable interval $\Delta\tau_{imp}$. The vertical line designates the instant of fuel portion injection start.

The superposition of waves in case of multiple injection may result both in amplification and damping of oscillations process. If the second injection is executed at the rear wave edge (pressure increase) or in the zone of minimum – the oscillations damping takes place. If the second injection is executed at the front (decreasing) wave edge or in the zone of maximum, the oscillations increase.

Figure 10 shows that at the interval $\Delta\tau_{imp}=3.6$ ms, after injection of the second portion, the maximal pressure oscillations range is 330 bar. At the interval $\Delta\tau_{imp}=5.5$ ms, the maximal range increases 1.45 times to 480 bar.

Figure 11 shows the results of estimation of the dependence of the injector rate Q of the second injection on the interval between injections. The first injection value is constant and amounts to $Q_1=16.5$ mg. The difference between the first and the second magnitudes of the injection rate is almost 2 times.

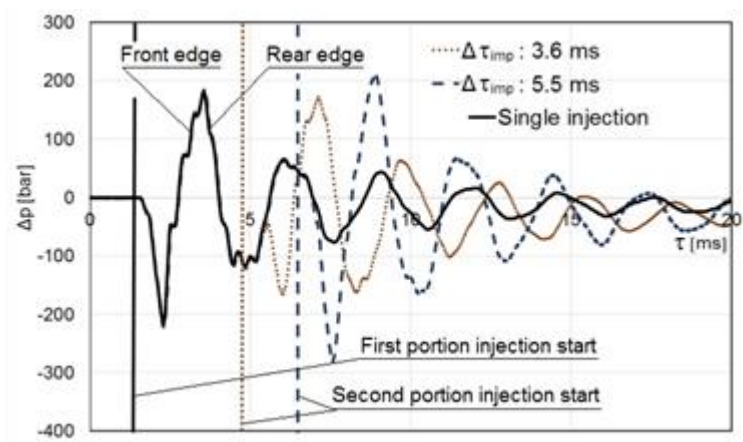


Figure 10 Pressure oscillations at the inlet of CRI No1 at various intervals between double injection
 $\Delta\tau_{imp}$ ($p_{ac}=1000$ bar)

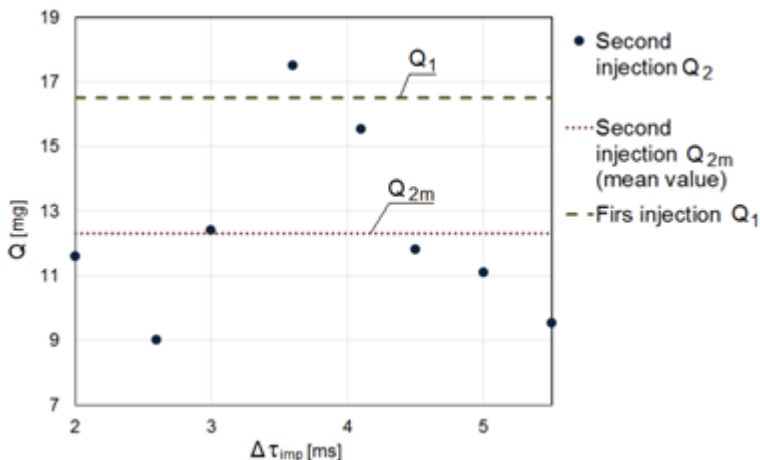


Figure 11 Fuel injection rate at various intervals between injections $\Delta\tau_{imp}$ ($p_{ac}=1000$ bar, $\tau_{imp}=0.6$ ms)

It should be mentioned that the average value of the second injector rate is considerably lower than of the first one.

Even if the beginning of the second injection is shifted removed from the first injection to the interval $\Delta\tau_{imp} = 50$ ms, the value of the second portion is 13.1 mg which is by 3.4 mg lower than the first one though the pressure oscillations of the first injection are damped completely during 50 ms.

This phenomenon has two explanations.

First, the pressure in the fuel accumulator drops after the first injection. The pressure deviation value is not large and according to data presented in Figures 3...4, amounts to 50 bar (depending on operation mode).

The second factor is voltage slump on the injectors power supply condenser. It follows from Figure 9 that forcing current of the second injection is by 2.5 A lower than the first one which promotes the longer opening of the injector.

In this way, modern injection system also makes stringent requirements to such parameters as fuel pressure control dynamics and charging the power supply condenser of the injectors.

Injection characteristic of the second fuel portion also depend on $\Delta\tau_{imp}$ because the pressure in the needle volume is interlinked with the pressure at the inlet of the CRI. For example, if the injection of the second fuel portion starts in the zone of pressure wave minimum and terminates in the zone of maximum (Figure 10), the fuel flow velocity through the spray holes will vary during the injection process from low to high.

Simulation was carried out to estimate the influence of fuel type and time interval $\Delta\tau$ (Figure 12) between control impulses of double injection on the value of the injection quantity of the second portion at pressures 2000...3000 bar.

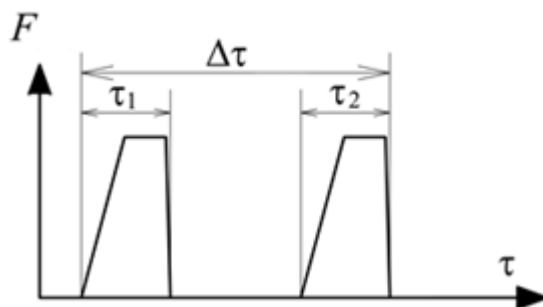


Figure 12 Control impulses modelled: F – injector electromagnet force, $\Delta\tau$ – time interval between control impulses, τ_1 – first control impulse duration, τ_2 – second control impulse duration

The simulation was carried out using the software package which is being developed in MADI.

The CRI No2 was selected as a subject of research, because it is providing a smaller pressure oscillations range.

The flow chart of the simulation is shown in Figure 13. Two equal control impulses were modeled ($\tau_1 = \tau_2$). Duration of the control impulses τ was selected such that the fuel quantity supplied during the first injection was $Q_1 \approx 3...4$ mg.

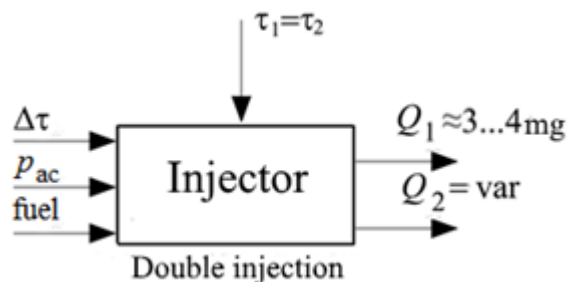


Figure 13 Test flow chart: Q_1 , Q_2 – injection rate values of the corresponding portions

Computation results of operation of the CRI No2 on diesel fuel are presented in Figure 14.

As was demonstrated during experimental tests (Figure 11), the reason of variation of injection rates versus $\Delta\tau$ were pressure oscillations at the inlet to the injector.

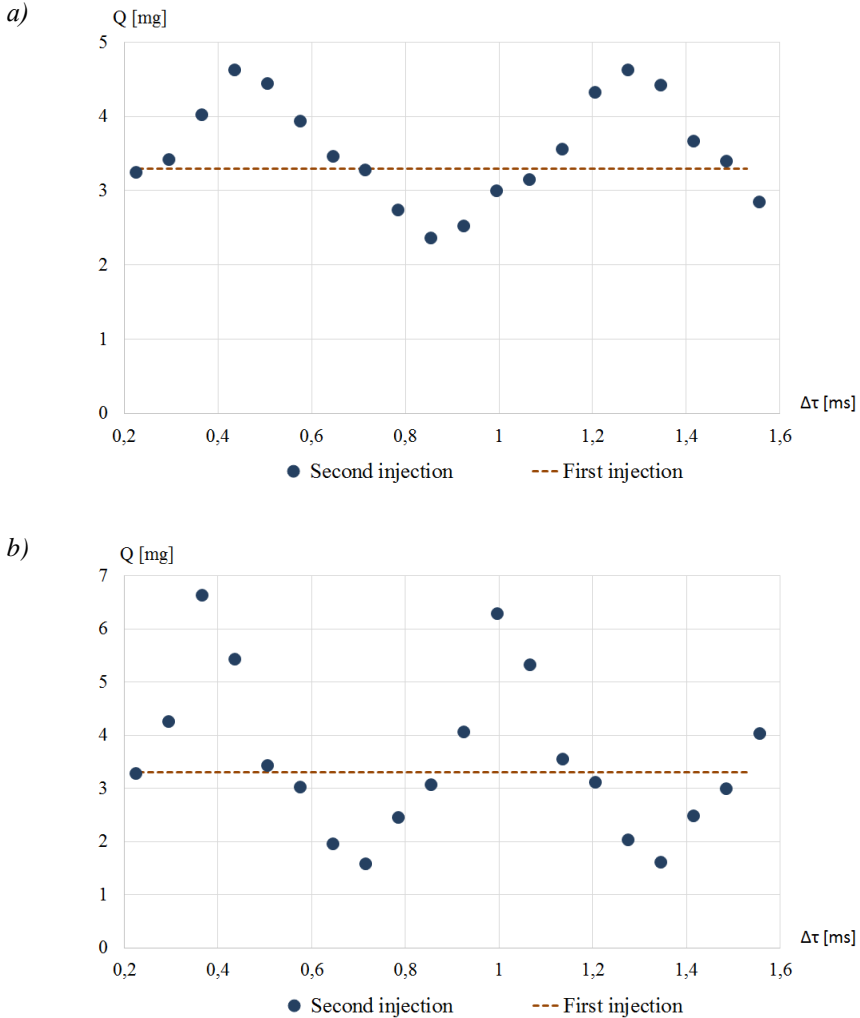


Figure 14 Injection rate Q_2 at different intervals between injections $\Delta\tau$ for diesel fuel ($Q_1 = 3.3$ mg):

$a - p_{ac} = 2000$ bar, $b - p_{ac} = 3000$ bar

When the pressure p_{ac} grows, the oscillation phenomenon and its impact on the working process increase. When operating on diesel fuel at pressure $p_{ac} = 2000$ bar, the spread in injection rates of the second portion is $Q_2 = 2.36 \dots 4.62$ mg, and at $p_{ac} = 3000$ bar $Q_2 = 1.58 \dots 6.63$ mg.

The results of imitation carried out for a more dense fuel corresponding to sunflower oil are presented in Figure 15.

The main difference of Figure 14 from Figure 15 is a faster attenuation of oscillations observed when passing to a more dense fuel. In case of $p_{ac} = 2000$ bar, the spread in injection rates of the second portion is $Q_2 = 2.96 \dots 4.21$ mg, and at $p_{ac} = 3000$ bar – $Q_2 = 2.42 \dots 5.50$ mg.

It is seen from comparison of calculated data (Figure 14 and Figure 15) that due to a higher hydraulic friction, the maximal pressure oscillations range is lower. This will have a positive effect on the control precision of the second portion of fuel injected.

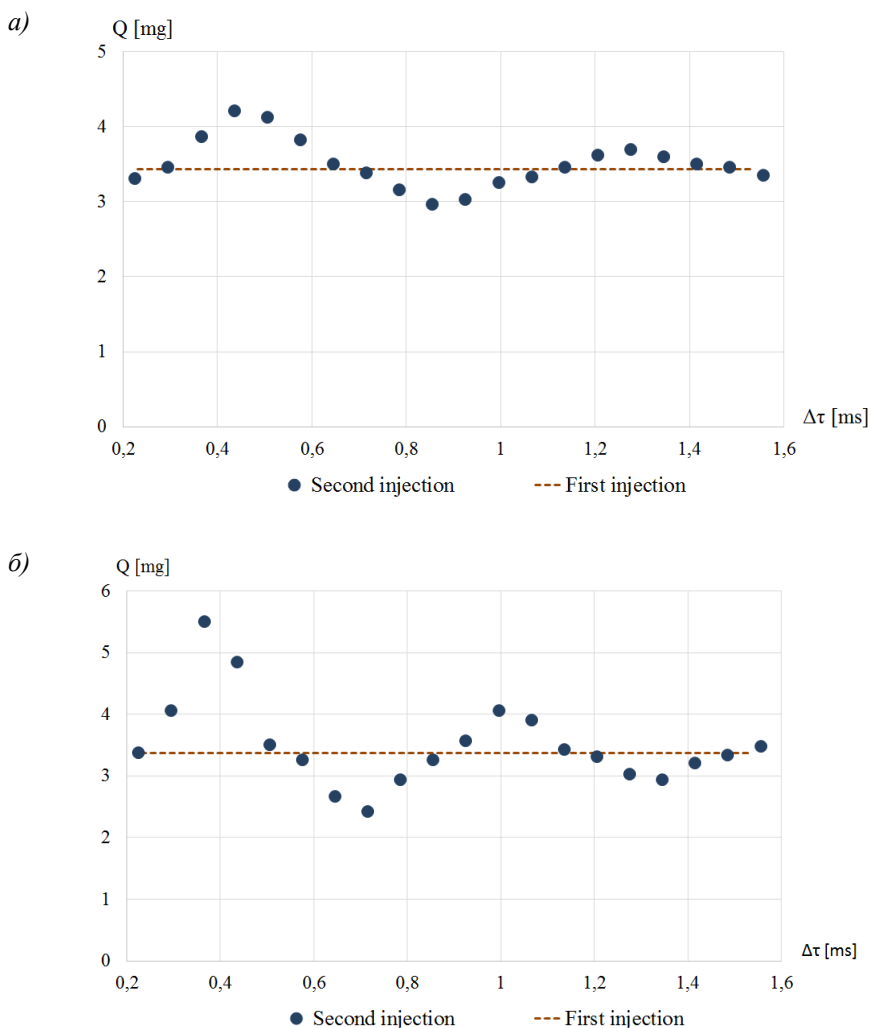


Figure 15 Injection rate Q_2 at different intervals between injections $\Delta\tau$ for a more dense fuel ($Q_1 = 3.4$ mg):

$$a - p_{ac} = 2000 \text{ bar}, b - p_{ac} = 3000 \text{ bar}$$

5. CONCLUSIONS

1. Fuel injection causes considerable pressure oscillations at the inlet of the injector. The oscillations range depends on: injection pressure, control impulse duration, fuel physical properties and injector design. One of the reasons of oscillations is hydraulic impact which takes place when the injector needle closes.

2. The pressure drop in the accumulator after preliminary injection (the amount of deviation of the pressure is 5 MPa depending on the mode) and the voltage drop across the capacitor of the power injector (the current boost of the second injection of 2.5 A less than the first) favors longer opening of injectors in case of next injection.
3. The presence of fuel accumulator integrated into the CR injector body decreases wave phenomenon related to fuel injection. During experiments with the injector CRI No2 having an integrated fuel accumulator ($p_{ac}=1000$ bar, $\tau_{imp}=0.6$ ms), the impulse amplitude at the inlet to the injector was 120 bar which is 3.3 times lower than in the injector CRI No1 having no fuel accumulator.
4. When the fuel accumulator pressure p_{ac} grows, the oscillation phenomenon and its impact on the working process increase. So when operating on diesel fuel at pressure $p_{ac}=2000$ bar, the spread in injection rates of the second portion is $Q_2 = 2.36 \dots 4.62$ mg, and at $p_{ac}=3000$ bar $Q_2 = 1.58 \dots 6.63$ mg.
5. When switching to a fuel with a higher viscosity due to the increase of the hydraulic friction there is a more rapid attenuation of the pressure oscillations caused by the preliminary injection. So when injector CRI No1 operates ($p_{ac}=1000$ bar, $\tau_{imp}=0.6$ ms) on sunflower oil the pressure oscillations range decreases from 40 MPa (operation on diesel fuel) to 25 MPa (operation on sunflower oil).

ACKNOWLEDGMENTS

Applied research and experimental developments are carried out with financial support of the state represented by the Ministry of Education and Science of the Russian Federation under the Agreement No 14.580.21.0002 of 27.07.2015, the Unique Identifier PNIER: RFMEFI58015X0002.

REFERENCES

- [1] Beirer, P. Experimental and numerical analysis of hydraulic circuit of a high pressure Common Rail diesel fuel injection system. Tampere: Tampere University of Technology, Finland, 2007, 198 p
- [2] Catania, A. E., Ferrari, A., Manno, M. Parametric Study of Hydraulic Layout Effects on Common-Rail Multiple Injections. 2005 Fall Technical Conference of the ASME ICED, Paper No. ICEF 2005-1288, Ottawa, Canada, 2005
- [3] Catania, A. E., Ferrari, A., Manno, M., Spessa, E. Experimental investigation of dynamics effects on multiple-injection Common Rail system performance. Journal of Engineering for Gas Turbines and Power, ASME. Volume 130. pp. 032806-032813
- [4] Leonhard, R., Warga, J., Pauer, T., Ruckle, M., Schnell, M. Solenoid Common Rail injector for 1800 bar. MTZ worldwide, February 2010, pp. 10-15
- [5] Pflaum, S., Wloka, J., Wachtmeister, G. : Emission reduction potential of 3000 bar Common Rail Injection and development trends. CIMAC Paper No. 195, CIMAC Congress Bergen, 2010
- [6] Shatrov, M. G., Golubkov, L. N., Dunin, A. U., Yakovenko, A. L., Dushkin, P. V. : Research of the injection pressure 2000 bar and more on diesel engine parameters. International Journal of Applied Research ISSN 0973-4562 Volume 10, Number 20 (2015) pp. 41098-41102

- [7] Sunwoo, K., Namhoon, C., Namhoon, C. Injection Rate Estimation of a Piezo-Actuated Injector. SAE Paper 2005-01-0911, USA, 2005
- [8] Why higher injection pressure saves fuel and also increases performance and torque, Bosch Media Service, 2013
- [9] Wloka, J. ; Pötsch, C. ; Wachtmeister, G. : Injection spray visualization for 3000 bar Diesel injection. 24th Conference of the Institute for Liquid Atomization and Spray Systems, 2011
- [10] Working best under pressure, Transport Engineer, November 2010, pp. 20-22.

APPLICATION AND DESIGN OF HYDRO TRANSMISSION FOR TRACTORS

Vanja Šušteršič, Dušan Gordić, Mladen Josijević, Vladimir Vukašinić¹

UDC:629.022

ABSTRACT: In the recent years, there has been a great progress in the development and practical application of hydro transmission in all industries. In particular, they are widely used in mobile machines in the construction, mining, agriculture and forestry for starting the working parts (manipulators) which perform technological operations and for driving power. The basic advantages and disadvantages of hydraulic power transmission are explained in this paper, with examples of application of both types - hydrostatic and hydrodynamic power transmission for tractors. Calculation of both types of hydraulic power transmission for tractors was made along with a 3D model based on the calculated size.

KEY WORDS: tractor, hydrostatic transmission, hydrodynamic transmission, 3D model

PRIMENA I PROJEKTOVANJE HIDRO TRANSMISIJA KOD TRAKTORA

REZIME: U poslednjih nekoliko godina došlo je do velikog napretka u razvoju i praktičnoj primeni hidro transmisija u svim granama privrede. Posebno se široko primenjuju u oblasti mobilnih mašina u građevinarstvu, rudarstvu, poljoprivredi i šumarstvu i to, kako za pokretanje radnih organa (manipulatora) koji izvode tehnološke operacije, tako i za pogone kretanja. U radu su objašnjene osnovne prednosti i nedostaci hidrauličnog prenosa snage, sa primerima primene oba tipa - hidrostatičkog i hidrodinamičkog prenosa snage kod traktora. Urađen je i proračun oba tipa hidrauličnih prenosnika snage kod traktora, sa 3D prikazom modela na osnovu proračunatih veličina.

KLJUČNE REČI: traktor, hidrostatička transmisija, hidrodinamička transmisija, 3D model

¹ Received: September 2016, Accepted September 2016, Available on line November 2016

Intentionally blank

APPLICATION AND DESIGN OF HYDRO TRANSMISSION FOR TRACTORS

*Vanja Šušteršič*¹, *Dušan Gordić*², *Mladen Josijević*³, *Vladimir Vukašinović*⁴

UDC: 629.022

1. INTRODUCTION

The production of tractors/ in the world began around 1858, and since then the evolution of the tractor significantly progressed. In Serbia, the first tractor was produced in 1949, which means 100 year after the first production of tractors in the world [1]. The development of transmissions for agricultural tractors has caused manual gearbox to change to hydrostatic, continuous, and eventually the electrical transmission. All these solutions have the aim to improve traction - dynamic characteristics optimize the agro-technical conditions and increase the degree of rationalization of production. In this way we are trying to find the most optimal solution, i.e. approach ideal pulling hyperbola.

In today's development trend of tractor transmissions there is an increasing application of so-called continuously variable transmissions which provides continuous power transfer depending on the operating conditions [2].

Tractors were initially made with small power motors and a small number of gears, but with the development of agriculture and the development of large farms, there was a need for larger and more powerful machines that are in possession of a larger number of gears and transmissions with more engine power. By observing the stage of development of tractor transmissions it can be seen that the mid-eighties of the twentieth century tractors had maximum speed beyond the standard 30 km/h, while the speed of tractors in nineties was around 40 km/h, which has become later a standard for higher power tractors. At the beginning of 21st century tractors with a maximum speed of 50 km/h appeared which set the new standards. Today, some manufacturers even offer special models of tractors with a maximum speed of over 60 km/h. Increasing the overall speed range, as well as number of requests for higher speed in the main operating range (4-12 km/h) and crawling speed (below 1 km/h), has led to a drastic increase in the number of gears from 4-5 in the sixties, to over 40 gears at the end of the twentieth century. In addition to the increased number of gears, the transmission had to become fully synchronized like the ability to change gears at full load. The purpose of a tractor defines his traction characteristics. The basic requirement is that in the exploitation range there is a number of gears that will provide different traction forces at different speeds, and that these speeds are in the context of technological speed for certain operations. In fact, sliding coefficient and the efficiency of the tractor must be within the limits laid down for the particular type of tractor.

¹ *Vanja Šušteršič, Prof., University of Kragujevac, Faculty of Engineering, Sestre Janjić 6, Kragujevac, vanjas@kg.ac.rs*

² *Dušan Gordić, Prof., University of Kragujevac, Faculty of Engineering, Sestre Janjić 6, gordic@kg.ac.rs*

³ *Mladen Josijević, Ph. D. student, University of Kragujevac, Faculty of Engineering, Sestre Janjić 6, mladenjosijevic@gmail.com*

⁴ *Vladimir Vukašinović, Ph. D. student, University of Kragujevac, Faculty of Engineering, Sestre Janjić 6, vladimir.vukasinovic@kg.ac.rs*

2. HYDROSTATIC TRANSMISSION

Hydrostatic transmissions have been around for a long time. A hydrostatic transmission consists of a pump hydraulically coupled to a hydraulic motor. It uses oil (hydraulic fluid medium) to transmit power from the power source to the driven mechanism. If the displacement of regulation pump and regulation engine is constant, hydrostatic transmission simply acts as a transmission that transmits power from the primary actuator to load. The main advantage of hydrostatic power transmission is the use of a variable displacement pump, regulating motors or both devices together, so that the speed, torque or power can be regulated.

Hydrostatic transmissions offer a number of advantages over other types of power transmission. Depending on their construction, hydrostatic transmissions:

- can transmit high power,
- exposed to low inertia,
- work effectively in a wide range of relations torque - speed,
- maintain a controlled speed regardless of the load within the structural limits,
- maintain the current speed exact opposite driving or braking loads,
- capable of transmitting one of the primary drivers of up to several locations, even if the position and orientation of the location change,
- can remain fixed and undamaged under full load at low power losses,
- do not slide at speed 0,
- provide a faster response in relation to the mechanical and electro-mechanical transmission,
- can provide dynamic braking.

Disadvantages of the hydrostatic system are the compressibility of fluids and fluid's viscosity that changes with temperature and pressure.

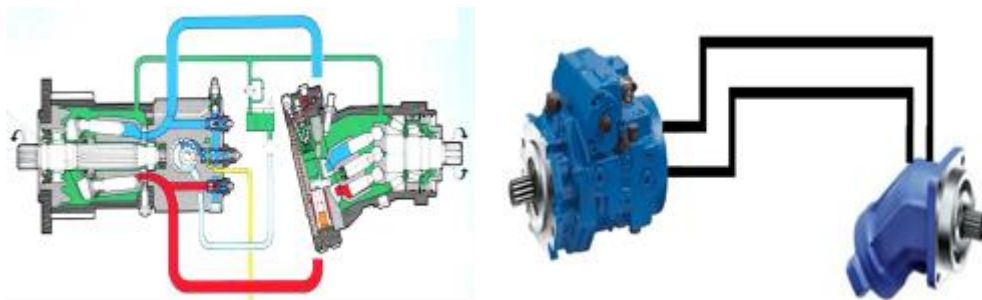


Figure 1 Hydrostatic transmission [3]

Wheel drive vehicles with hydrostatic transmission design can be performed in several ways. The first way, and also the simplest, is through construction pumps and motors in the same housing (Figure 2a) where the drive torque is applied to the wheels through a differential with an additional reduction in the wheels. Another way is with pump that drives two hydraulic motors attached to the gear wheels (powered two-wheel vehicles) (Figure 2b), and the third way is the one that is used to drive the vehicle on all four wheels being driven where pump supplies hydraulic motors with energy (the pump is built into the wheels of the vehicle with planetary gear unit) (Figure 2c) [4].

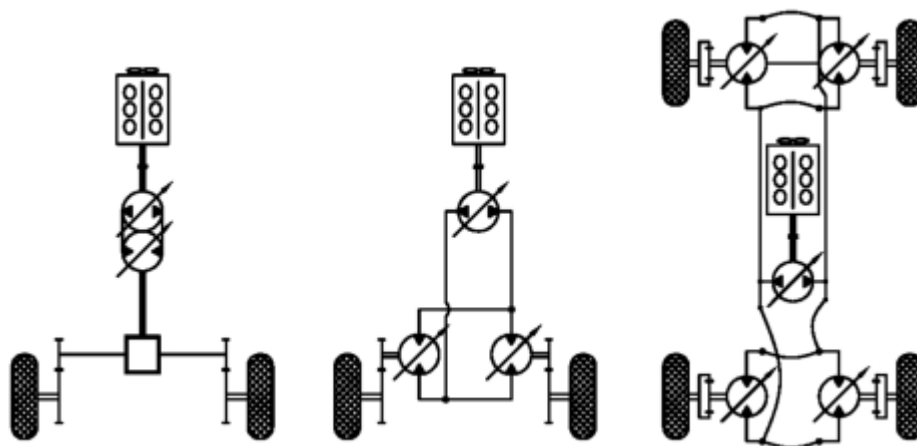


Figure 2 Variants of the vehicle wheel drive with a hydrostatic transmission:
 a) construction of pumps and motors in the same housing, b) two wheel drive,
 c) four wheel drive [4]

The tractor mainly uses pumps and motors axial piston-type with tilting plate. Further development of continuously variable transmissions can be achieved with the use of friction and electrical continuously power transmissions, but also of a hybrid drive, with diesel engine and an electric motor powered by electric batteries and a generator.

In the last years, modern efficient tractors have been distinguished by continuous variable transmissions (CVT) which enabled infinite number of tractor speeds. A split power (hybrid transmission or CVT) improves the efficiency of a hydrostatic transmission while retaining the advantage of continuous variability. In the hybrid transmission presented by Figure 3, power is partially transmitted mechanically and partially - hydrostatically. For example, the Fendt Vario transmission is a hydrostatic-mechanical power split drive. With the speed increase, the share of the mechanical power transmitted through the planetary set increases. The hydrostatic motor, which can be swung 45 degrees, and a high operating pressure of max. 550 bars ensure exceptional efficiency.

Varying the displacement of the pump provides a continuously variable speed ratio. At the startup and with low output speeds, most of the power is transmitted via the hydrostatic drive. As the output speed continues to increase, an increasingly large percentage of the power is transmitted mechanically and a smaller percentage is transmitted hydrostatically. Thus, as power demand rises, an increasing portion of the power is transmitted via the more efficient mechanical drive. The range transmission permits efficient operation at low field speeds and also at high transport speeds. The low range of this transmission provides speeds of 0.03 to 21 km/h, while the high range provides speeds of 0.03 to 50 km/h and reverse speeds of 0.03 to 38 km/h [6].

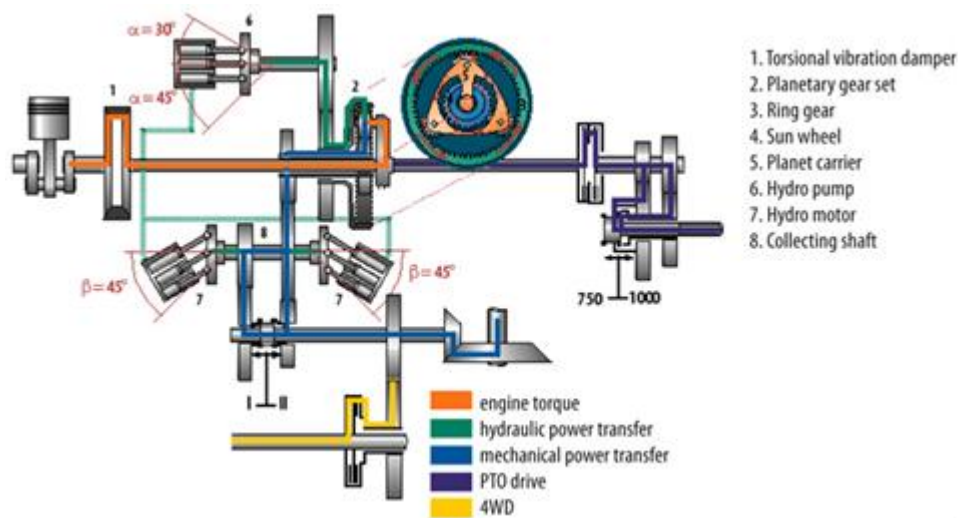


Figure 3 The Fendt Vario transmission [5]

In addition to previously mentioned Fendt Vario transmission, today there are two construction solutions for standard agricultural tractors on the market. These are „S- Matic“ CVT/CVX gear from factory „Steyr“ and „Eccom“ producer „ZF“. These transmissions are currently installed in tractors „Case –IH“ and „Case- Steyr“, and the tractor „John Deere“ and „Deutz – Fahr“.

2.1 Calculation of hydrostatic transmission

The calculation was done for the hydrostatic transmission which is applied to wheeled tractors Fendt 313 Vario.

The initial data were:

- the total mass of the tractor: $m_0 = 10000 \text{ kg}$
- load weight: $m_l = 3500 \text{ kg}$
- dynamic wheel radius: $r_d = 0,685 \text{ m}$
- engine power: $N = 90 \text{ kW}$
- pump speed: $n_p = 4500 \text{ min}^{-1}$
- maximum operating speed: $v_{R_{\max}} = 11 \text{ km/h}$
- maximum transport speed: $v_{T_{\max}} = 45 \text{ km/h}$
- the adhesion coefficient: $\phi = 0,8$
- the resistance coefficient: $f = 0,03$
- ratio: $i_G = 18,79$

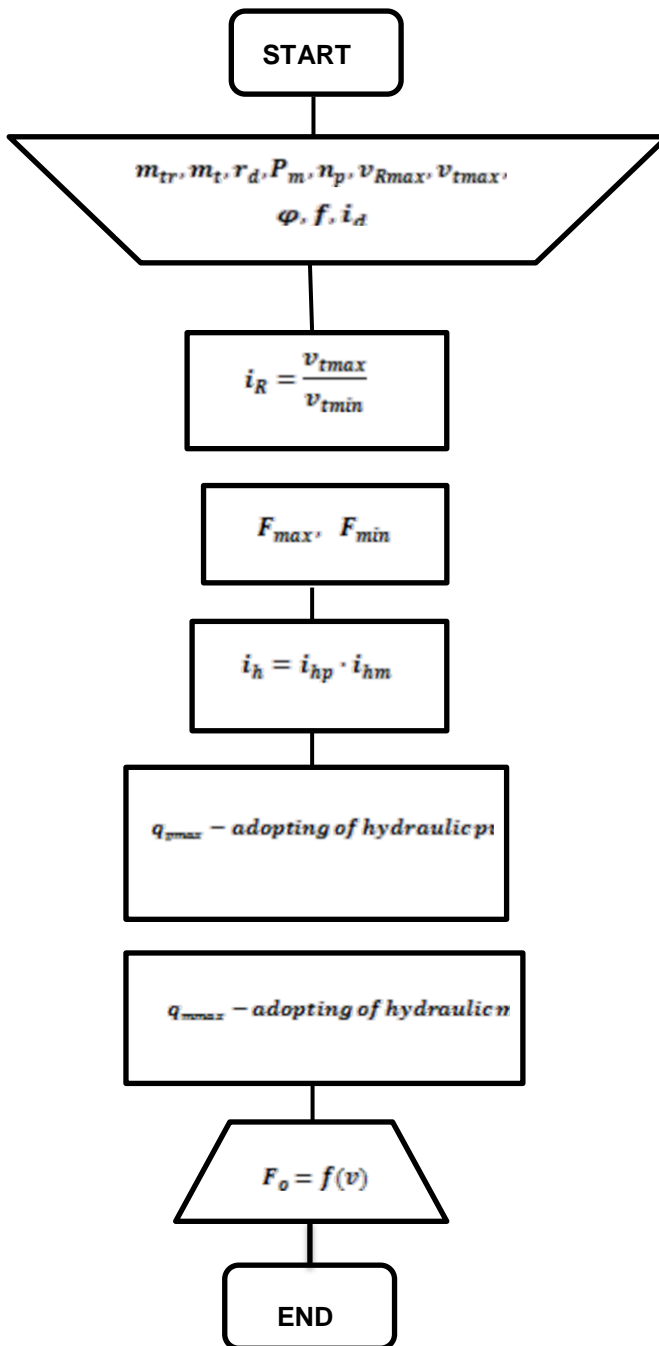


Figure 4 Algorithm for calculation of hydrostatic transmission

The figure 4 shows an algorithm for calculation of hydrostatic transmission. The calculation consists of determining the traction (Figure 5), according to the maximum specific flow rate of the hydraulic pump and hydraulic motor.

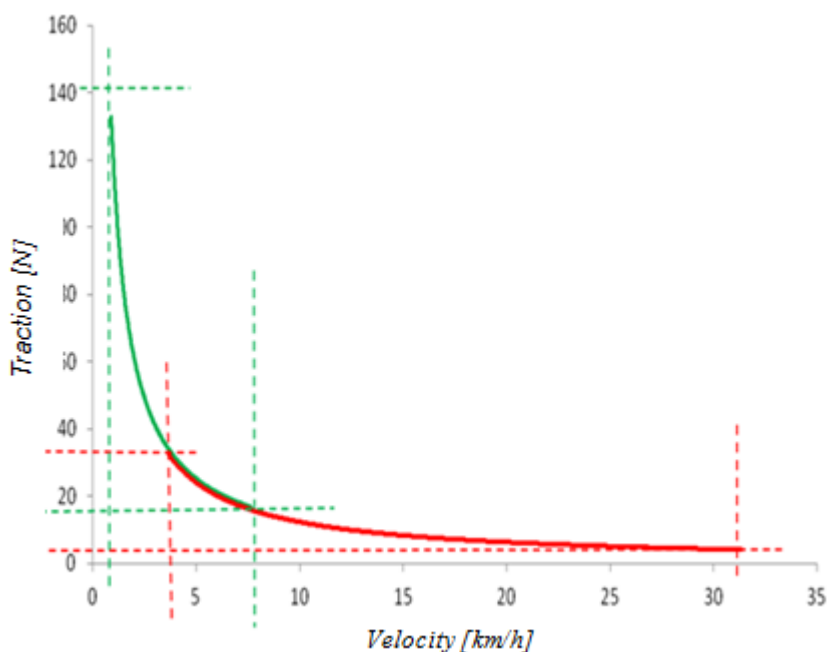


Figure 5 Chart of depending on the velocity-traction

3. HYDRODYNAMIC TRANSMISSION

Hydrodynamic power transmission for tractors occurs only in combination with mechanical or hydrostatic components. The basis of hydrodynamic transmission consists of a hydrodynamic coupling (Figure 6) or hydrodynamic torque converter.

Although it was shown that tractors with a hydrodynamic coupling have higher productivity of 12 to 20% comparing to the tractor without it, while the hydrodynamic torque converter on tractors have no greater application due to high prices, the complexity of the structure and relatively poor output parameters. Most frequently use can be found on the US market, comparing to Europe where it can be rarely found.

Due to fundamental differences in principle of action and properties, hydrostatic and hydrodynamic transmissions are separately examined. However, it is possible to make some basic comparisons:

a) The fact that the hydrostatic power transmission is based on pressure fluids, causes complete tightness of these transmission, which requires a good sealing and high quality processing. Bearing in mind that the transfer of high power hydrostatic gear can only be done effectively at high pressure (250-300 bar), the problem of sealing the required quality of processing represents major drawback of hydrostatic transmission. In the hydrodynamic transmission, quality of processing is not the most important condition of quality power transmission, and considering the pressures in these transmission is low, sealing is easily solved. The power that can be transmitted by hydrodynamic transmission is practically only limited by durability of materials (considering the present centrifugal forces acting on the rotating parts of these transmission).

b) Comparison based on dimensions give favors to hydrostatic transmission, particularly in the transfer of small forces.

c) As regards the level of efficiency, its change is favorable with the hydrostatic transmission, or on the side of the hydrodynamic transmission, the advantage is that the moment and the speed automatically adjust operating conditions (load output shaft). When hydrostatic transmission regulation is made outside impulses.

d) Elements of hydrodynamic transmission does not require special maintenance, whereas for hydrostatic it is essential [7].

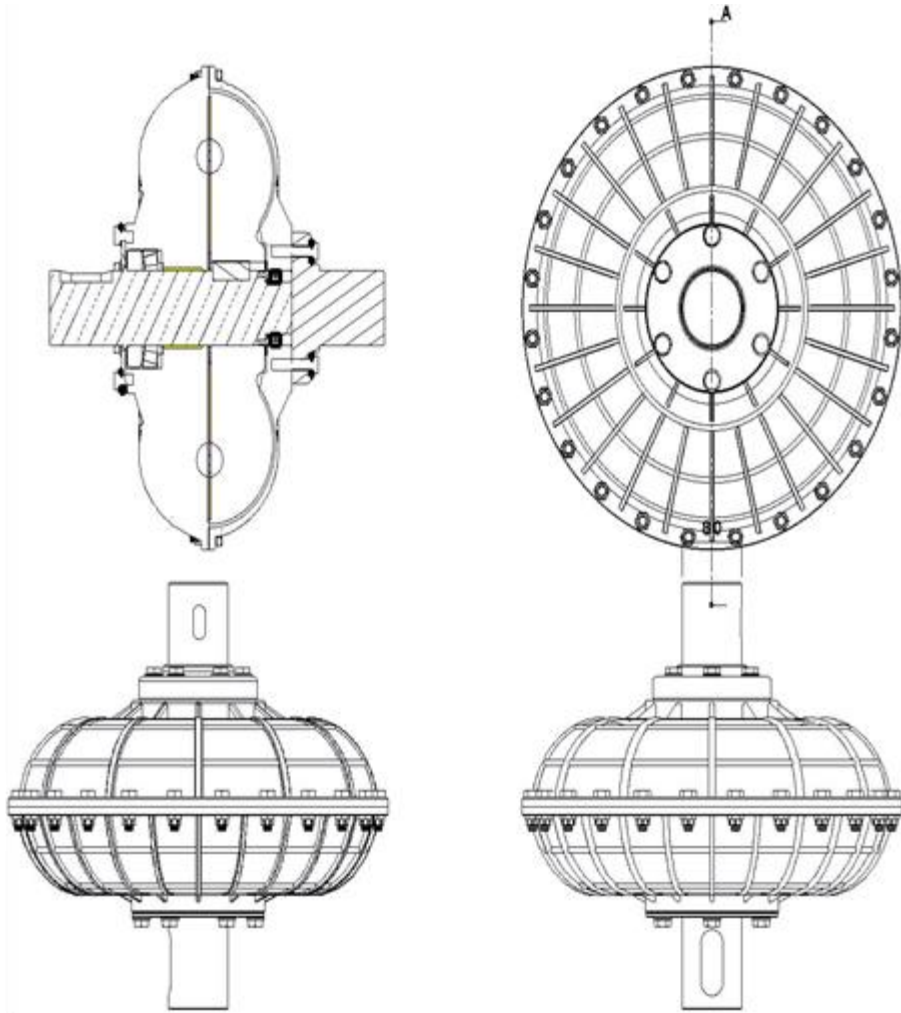
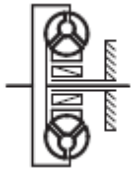
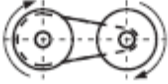

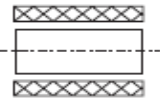


Figure 6 Hydrodynamic coupling

In table 1 shows the basic differences, advantages and disadvantages of transmissions used in tractors.

Table 1 Important physical principles of continuously variable transmissions for vehicle drives [8]

Type of CVT	Principle of energy Transmission	Ratio control	Application	Efficiency
1. 	Mass forces at pump and turbine	Usually automatically by load	Important for pass. cars and construction machinery	poor
2. 	Traction forces within friction contacts	Radius of traction force	Important for passenger cars	excellent
3. 	Hydrostatic forces at pumps and motors	Displacement of the units	Important for mobile machinery	moderate
4. 	Electro-magnetic forces at generators and motors	Frequency of current or electric flux or load	Upcoming	moderate

3.1 Calculation of hydrodynamic transmission

Calculation of hydrodynamic transmissions is done by tractor John Deere 7310R [9]. The input data are:

- Power: $P_p = 250,8 \text{ kW}$
- Speed drive: $n = 1900 \text{ min}^{-1}$
- Impeller speed: $n_p = 1900 \text{ min}^{-1}$
- Hydraulic oil: 850 kg/m^3 , at $t = 20 \text{ }^\circ\text{C}$, working temperature $t = 55 \text{ }^\circ\text{C}$

The figure 7 shows an algorithm for calculation of hydrodynamic transmission, and in the figure 8 3D model of this transmission is shown.

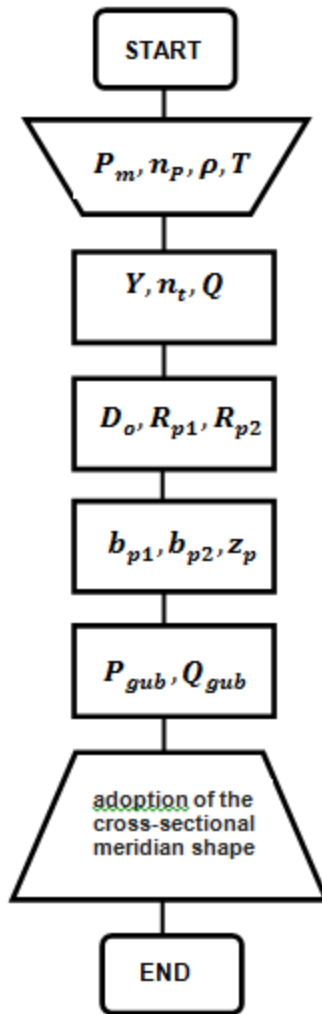


Figure 7 Algorithm for calculation of hydrodynamic transmission



Figure 8 3D model of hydrodynamic coupling

4. CONCLUSION

In many countries, about 40 to 50 % of the total investment in agricultural mechanization is invested in tractors. Constructional features of tractors used in high-income countries in the last 30 years have changed significantly. Western European and North American farmers require modern, so-called , "high - tech" tractors, equipped with the latest technical advances that enable high productivity and efficiency. More and more attention is paid to the ergonomics of the tractor, and the tractor impact on the environment.

The use of hydrostatic and hydrodynamic transmissions will always find application in the transfer of rotary motion which requires safe, accurate and reliable operation of the power transmission system. Construction, energy, agriculture, transport and other branches already know how to use the benefits of such widely used power transmission. Daily improvement and increasing the overall efficiency level, as well as combining with other power transmission, open up a wide field of application of such power transmission systems with emphasis on application of composite materials with high resistance, and also it reduction the weight of these transmission.

REFERENCES

- [1] Obradović D., Petrović P., Dumanović Z., Kresović B.: „Chronology of the development trend of production of tractors in Serbia ” , Agricultural Engineering , University of Belgrade , Faculty of Agriculture, year XXXVI, No. 1, pp.1-10, December 2011. ISSN 0554-5587 (in Serbian)
- [2] Petrović P., Obradović D.: „The analysis of development trend of tractor transmissions from the aspect of improvement of pulling - dynamic characteristics”, Agricultural Engineering, year XXXI, No 1, pp. 91-99, December 2006, (in Serbian)
- [3] Karl Erik Rydberg: “Hydrostatic drives in heavy mobile machinery - New concepts and development trends”, Linkoping University, 1997
- [4] Gregov G.: “Contribution to the research of modeling a hydrostatic transmission vehicle in the forest”, Faculty of Engineering, Rijeka, 2012. (in Serbian)
- [5] <http://www.fendt.com/> [available 20.08.2016.]
- [6] Goering E. C., Hansen C. A.: “Engine and Tractor Power”, American Society of Agricultural and Biological Engineers, September 2006
- [7] V. Kelić: “Hydropower transmission”, Scientific Book , Belgrade, 1989, (in Serbian)
- [8] Renius Th. K., Recsh R.: “Continuously Variable Tractor Transmissions”, Agricultural Equipment Technology Conference, Louisville, Kentucky, USA, 2005
- [9] <https://www.deere.com/> [available 20.08.2016.]

Intentionally blank

A NOVEL APPROACH FOR SOLVING GEAR TRAIN OPTIMIZATION PROBLEM

Nenad Kostić, Nenad Marjanović, Nenad Petrović¹

UDC:629.021

ABSTRACT: Gear train optimization is a constant subject of research with the goals of its adequate and justified use. One of the more important segments of optimization is the criteria of gear train volume. This paper is oriented on the analysis of the problem of decreasing gear train volume from a gear shaft axis position aspect. A heuristic approach has been developed for positioning shaft axes along a golden spiral contour, and the methodology for this alternative solution of optimization problems was defined. This approach represents an imitation of natural occurrences and development processes in nature. Nature itself achieves optimal processes, therefore this research started under the assumption of convergence towards optima. The process is verified on examples as functional, and results were compared to optimal solutions from literature. Achieved results of volume decrease are directly linked to savings, not only on space, but on housing material for the gear train, costs, speed of forming construction documentation, etc.

KEY WORDS: gear train, optimization, golden spiral, heuristic, novel method

NOVI PRISTUP REŠAVANJU OPTIMIZACIJE ZUPČASTIH PRENOSNIKA

REZIME: Optimizacija reduktora predstavlja stalnu temu istraživanja u cilju njegove adekvatne i opravdane primene. Jedan od značajnijih segmenata optimizacije jeste kriterijum zapremine reduktora. Ovo istraživanje orijentisano je na analizu problema smanjenja zapremine reduktora sa aspekta pozicije osa vratila zupčanika reduktora. Razvijen je heuristički pristup pozicioniranja osa vratila po konturi zlatne spirale i definisana je metodologija ovakvog alternativnog rešenja optimizacionog problema. Ovakav pristup predstavlja oponašanje prirodnih pojava i procesa razvoja u prirodi. Priroda sama po sebi postiže optimalne procese, tako da je ovo istraživanje započeto pod pretpostavkom konvergencije ka optimumu. Postupak je verifikovan na primerima, kao funkcionalan i rezultati su upoređeni sa optimalnim rešenjima iz literature. Dobijeni rezultati smanjenja zapremine direktno su povezani sa uštedama, ne samo u prostoru, već i u materijalu kućišta reduktora, troškovima, brzini formiranja konstrukcione dokumentacije i sl.

KLJUČNE REČI: zupčasti prenosnici, optimizacija, zlatna spirala, heuristika, nova metoda

¹ *Received: September 2016, Accepted October 2016, Available on line November 2015*

Intentionally blank

A NOVEL APPROACH FOR SOLVING GEAR TRAIN OPTIMIZATION PROBLEM

*Nenad Kostić*¹, *Nenad Marjanović*², *Nenad Petrović*³

UDC: 629.021

1. INTRODUCTION

From a research and practical aspect, there is a need for constant improvement in theoretical and practical segments in order to justify the use of gear trains. As a basic problem is achieving better working characteristics, performances, in terms of mass, volume costs, etc. Chong et al. [1] presented a general methodology for optimizing gear ratios, sizes and housing volume for multi-stage gear trains in preliminary design phases. Marjanovic et al. [2] developed a practical approach to optimizing gear trains with spur gears based on a selection matrix of optimal materials, gear ratios and shaft axes positions. Golabi et al [3] presented gear train volume/weight minimization optimizing single and multistage gear trains' gear ratios. Mendi et al. [4] aimed to optimize gear train component dimensions to achieve minimal volume comparing GA results to analytic method parameter volume. Savsani et al. [5] described gear train weight optimization comparing various optimization methods to genetic algorithm (GA) result values. Gologlu and Zeyveli [6] performed preliminary design automation through optimization of gear parameters and properties using a GA based approach. Pomrehn and Papalambros, [7] optimized gear train volume varying gear thicknesses, distances between centers, pitch diameters, number of teeth, ratios, etc. for a specific four stage setup. Deb and Jain [8] used similar principles for optimizing multi-speed gearboxes using multi-objective evolutionary algorithm optimizing volume in relation to power.

In order to facilitate improvement in this field, a great deal of experience and use of novel and alternative methods is required. Optimization presents a way of effectively achieving desired characteristics of gear trains. This paper is concentrated only on gear trains with parallel shaft axes. Aside from knowing reducer construction, the processes and method of optimization, it is necessary to develop a mathematical model which can be representative of the problem, and improve performances. Modern approaches of solving this problem represents the use of a heuristic approach, as an alternative to optimization. A heuristic approach allows for achieving adequately optimal solutions with having very little input data.

Motivation for this research is to find a means, and volume optimization method for gear trains using a heuristic approach, where a minimal amount of input data is necessary in order to form a universal method and approach for solving this specific problem for any gear train of this type. Furthermore this method should lead to achieving minimal volume, and with that a lower mass of the construction, smaller dimensions,

¹ *Nenad Kostić, research assist., University of Kragujevac, Faculty of Engineering, Sestre Janjić 6, 34000 Kragujevac, nkostic@kg.ac.rs*

² *Nenad Marjanović, Ph. D prof., University of Kragujevac, Faculty of Engineering, Sestre Janjić 6, 34000 Kragujevac, nesam@kg.ac.rs*

³ *Nenad Petrović, Assist., University of Kragujevac, Faculty of Engineering, Sestre Janjić 6, 34000 Kragujevac, npetrovic@kg.ac.rs*

savings on materials, expenses and other benefits. The realization of this problem is oriented on mimicking natural occurrences. This heuristic approach considers using a golden spiral, which represents the correlation of growth and development in nature, with the assumption that it would have the same effect in the process of gear train design.

2. PROBLEM DEFINITION

Gear trains with parallel shaft axes are commonly designed to have all axes in the same plane. This is most frequently the horizontal plane. Such a setup of gears takes up a large space which could be decreased by optimizing the gear train. An optimal solution defines a new position of axes which in turn causes the decrease in overall volume. Gear train volume is defined by the product of length width and height based on which a mathematical model is created. As the width can be considered constant due to calculated values of gear dimensions and other construction dimensions, the optimization problem is reduced to the optimization of area as a product of length (L) and height (H) of the gear train. Optimal volume can be achieved by forming a mathematical model, as was done in some research papers [1-3, 7]. There is a tendency to avoid complex mathematics which represents the goal function and constraints. For this problem it is possible to achieve an optimal solution by combining the trajectory of the golden spiral and positions of the gear train axes. By placing the axes on the contour of the golden spiral it is possible to achieve an alternative solution for minimizing gear train volume, or more precisely minimizing its area in the plane normal to the shafts.

2.1 Golden spiral definition

Growth and development of natural structures and processes always has the same, unique dependency. This dependency can be mathematically formulated and presented by the golden section (1.6180339887), golden angle (137.508°), and golden spiral. The golden spiral, due to its complexity, can be approximated by a line which connects the corners of tiles which are the size of the Fibonacci sequence (1, 1, 2, 3, 5, 8, 13, 21...). Natural dependencies formed in a spiral as the Fibonacci tiles are presented in picture 1, where a correlation can be easily seen. The Fibonacci spiral has a very small divergence from the golden spiral, and it is easy to use. This is the reason for the golden spiral being commonly considered as the Fibonacci spiral, which is also the case in this paper.

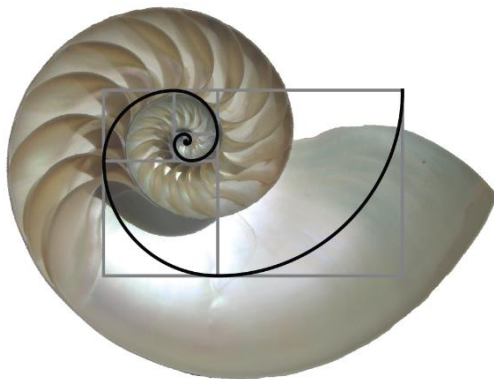


Figure 1 Fibonacci tiling and spiral found in nature

The golden spiral has a large influence as it represents a natural solution and depicts natural occurrences. The use of these occurrences from nature presents an analogy to natural solutions. When applied, these solutions seem completely natural and logical, while their possible implementation is not always easily noticed.

2.2 A novel approach (novel method)

This research is oriented towards analyzing the problem of minimizing gear train volume from a shaft axes position angle aspect. A heuristic approach to positioning axes along the contour of a golden spiral was developed, and the methodology of such an alternative solution for optimization is defined. This approach represents mimicking natural occurrences and processes of development in nature. Nature in itself achieves optimal processes, therefore this research was started under the hypothesis of it converging towards an optimum.

Forming a golden spiral is done according to the distance between two axes. In order to avoid overlap among gear train elements it is necessary for the distance between the first gear pairs axes be the same as the diagonal of the third tile of the Fibonacci spiral (1).

$$a_1 = f_3 \sqrt{2} \tag{1}$$

where:

a_1 - distance between axes of the first gear pair,

f_3 - size of the side of the third Fibonacci tile.

The presented equation (1) is the first condition of this approach. The rest of the shaft axes are placed along the golden spiral in order. This approach can be applied to all multi stage gear trains, regardless of the number of stages. A planar representation of how a multistage gear train design should look is shown in picture 2.

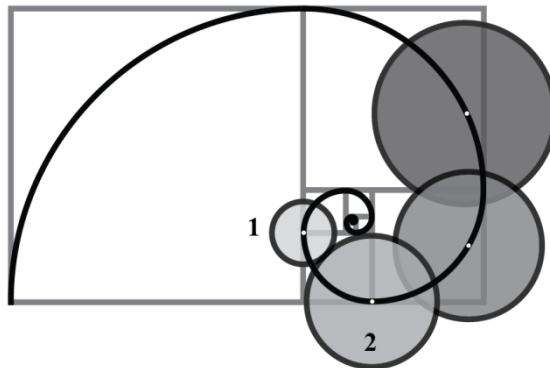


Figure 2 Planar view of gear placement along Golden spiral

The number of stages of the gear train does not influence the methodology of approach, as in can be seen in picture 2. In case there is overlap of gear train elements in this setup, the starting point of the first gear axes should be moved to point 2 (Picture 2).

As the width of the reducer is constant due to calculated values, the volume depends exclusively on the length and height of the gear train. This reduces the volume optimization problem to a planar area minimization problem. In the case of a contemporary concept the housing is a lot larger than when the axes are placed at different angles from the horizontal plane. The complete methodology of gear train volume optimization is developed based on this fact. A simplified diagram of which angles are optimized is shown in picture 3.

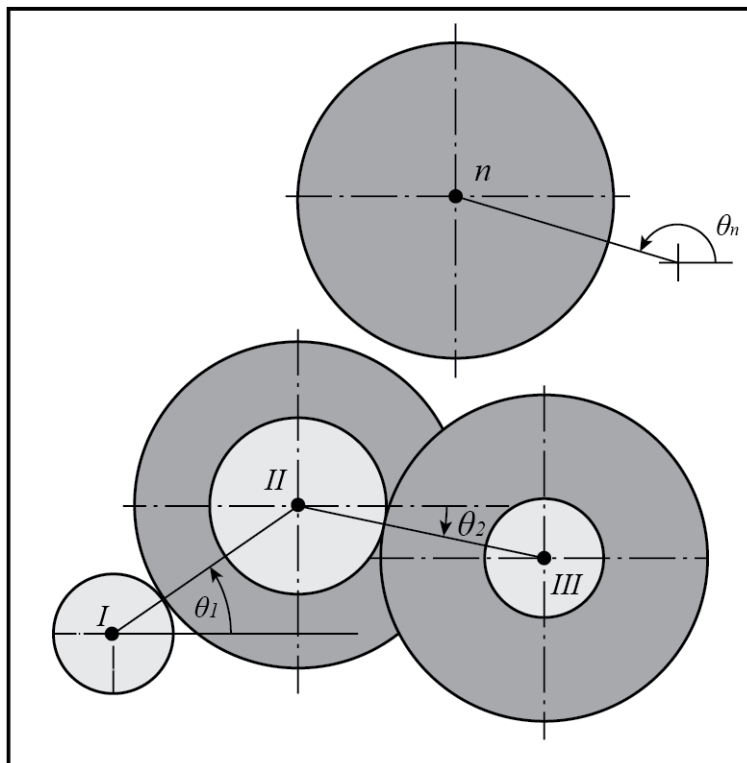


Figure 3 Gear train optimization of axes angles for gear train with n gear pairs

The approach is completely original and therefore is presented as a novel method for solving gear train volume optimization problems. The benefits of this methodology are that there are no complex equations which define the mathematical model, there is no need for using optimization software, and the solution is achieved in a quick and simple manner. The methodology is generalized, meaning that it can be used on all gear trains with parallel shaft axes.

3. TEST EXAMPLES

In order to verify this research, and its practical application verification was conducted on examples from literature. Two examples were used, where example 1 [2] is a

two stage, and example 2 [1] is a four stage gear train. For input data gear diameters are necessary. All gear train data is shown in table 1.

Table 1 Input values for testing for two examples

Stage	Example 1(2 stage)			Example 2 (4 stage)			
	1	2		1	2	3	4
Module (mm)	2	3		1.5	2	3	4
Number of teeth in pinion	20	23		14	18	20	25
Number of teeth in gear	83	67		77	79	74	82
Pitch diameter of pinion (mm)	40	69		21	36	60	100
Pitch diameter of gear (mm)	166	201		115.5	158	222	328
Face width (mm)	103	135		68.25	97	141	214
Net length, height, width	388.5	231	110.6	724.75	358	153	

Presented values in table 1 are dimensions of the gear train and using these values initial volume of the conventional setup can be calculated. Gear train volume is calculated with clearances of 15mm on all sides from the gear train housing and between gear train elements, and the calculations are done according to [2]. Initial volume of the two stage gear train (Example1) is 9 925 631.1mm³, and the four stage (Example 2) is 39 697 456.5mm³. Picture 4 shows concepts of example 1 and example 2, for the conventional and optimal shaft axes positions.

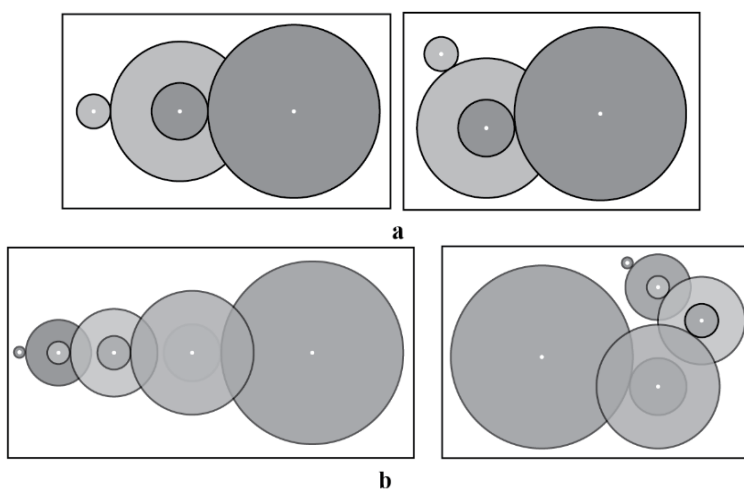


Figure 4 Conventional and optimal concepts a) Example 1; b) Example 2

Optimal gear train volume for Example 1 is 8 874 585.6 mm³, and for Example 2 is 31 767 763.4 mm³. These values are achieved by optimization and need to be compared to volumes achieved using the golden spiral approach, using the same width of each gear train respectively.

4. RESULTS

In order to achieve an optimal solution a large number of complex equations needs to be developed, which create the mathematical model. The optimization method needs to be utilized and adapted to the problem or adapt the problem to the optimization method. All this resents a long and arduous process in which there is always room for error and wrong conclusions. The idea of the golden spiral approach is that that process is avoided, and still achieve acceptable, improved solutions. These solutions can be treated as optimal as there is a minimal effort put into them, with a minimal amount of input information, achieving notable benefits and minimizing volume.

For achieving results, table one is used for optimal concepts. The first step is to have the first gear pair placed freely in the vertical plate, after that a golden (Fibonacci) spiral is constructed, so that the diagonal od the third Fibonacci tile is the distance between the shaft axes of the first gear pair. The other axes are placed along the spiral contour in order. The improvements which can be achieved through optimization in this case depend mainly on the diameters of the gear pairs.

With conventional optimization approaches shaft axes (the planes in which they lay) in relation to the horizontal plane are at a specific angle, and the optimal area and volume can be achieved using more than one angular setup. For the golden spiral approach it is not possible to change angles.

The golden spiral approach comparison to optimal solutions is in calculation the areas and volumes of both and comparing their deviations. Values for the conventional, optimal [2], and golden spiral dimensions and volumes are given in Table 2 for both examples.

Table 2 Values for conventional, optimal, and golden spiral designs

		L [mm]	H [mm]	B [mm]	V [mm ³]
Conventional	Two stage gear train	388.5	231	110.6	9925631.1
	Four stage gear train	724.8	358	153	39700195.2
Optimal	Two stage gear train	347.4	231	110.6	8875583.6
	Four stage gear train	555.6	373.7	153	31767041.2
Golden spiral	Two stage gear train	347.4	231.1	110.6	8879425.9
	Four stage gear train	559.7	384.2	153	32900621.2

From table 2 it is obvious that values achieved using the new approach are very close to optimal values, which directly indicates the validity of the new developed approach. Optimal solutions have values in acceptable ranges for the same value of volume, as shown in picture 5.

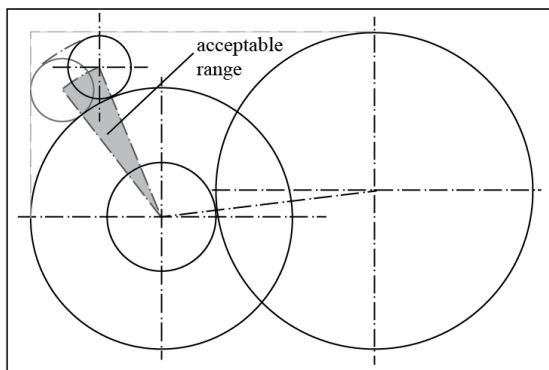


Figure 5 Acceptable angle ranges for the optimal solution of Example 1

For solutions achieved using the new approach the use of the golden spiral has a singular solution. A schematic visualization of the new solutions is shown in picture 6.

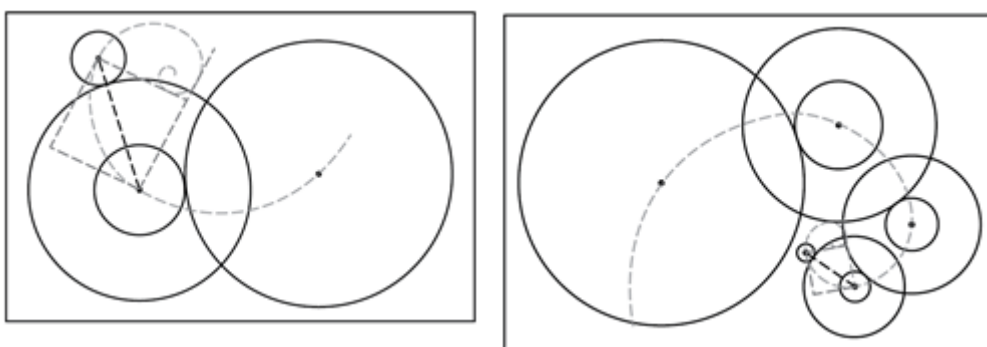


Figure 6 Optimal gear train setups using new method

Based on achieved results and table 2 it can be concluded that the reduced gear train volume by optimization gives a 10.58% decrease from the conventional design, while the new approach yields a 10.54% decrease for Example 1. The decrease on volume for Example 2 using optimization is 19.98%, while the new approach gives a 17.13% decrease.

It is obvious that optimization yields somewhat better results; however the effort put into achieving those results is much greater than for the novel approach. As an optimal solution is one which is achieved with the least amount of effort while achieving maximal gain, the novel approach can be treated as optimal. This methodology presents an alternative for practical use in gear train design due to its simplicity and benefits in terms of volume minimization.

5. CONCLUSIONS

The novel approach presented by this paper has been verified on examples, as functional and the results have been compared to optimal solutions from literature.

The optimization process requires the development of numerous equations and constraints for the mathematical model, whose number increases even further with the number of stages of the gear train which is optimized. Using the golden spiral novel approach the complex mathematic model is avoided all together, thereby shortening the time needed to develop the design of such a setup and minimizing the risk of error in the process. In addition to these benefits, the implementation of the novel method into software is very simple as opposed to optimization methods which require the creation of, or modification of existing software in order to use.

Results achieved using the novel method is very close in values to optimal solutions, and their deviation in terms of percentage is acceptable for engineering practice. Given the simplification of achieving an improved design concept by using the novel approach, the difference in volume minimization compared to optimization is negligible.

Achieved results of minimized volume are directly linked to savings, not only in space used, but also in material for the gear train housing, costs, speed of forming design documentation, etc.

REFERENCES

- [1] Chong, T. H., Bae, I., and Park, G.-J., 2002, "A new and generalized methodology to design multi-stage gear drives by integrating the dimensional and the configuration design process," *Mechanism and Machine Theory*, 37(3), pp. 295-310
- [2] Marjanovic, N., Isailovic, B., Marjanovic, V., Milojevic, Z., Blagojevic, M., and Bojic, M., 2012, "A practical approach to the optimization of gear trains with spur gears," *Mechanism and Machine Theory*, 53, pp. 1-16
- [3] Golabi, S. i., Fesharaki, J. J., and Yazdipoor, M., 2014, "Gear train optimization based on minimum volume/weight design," *Mechanism and Machine Theory*, 73, pp. 197-217.
- [4] Mendi, F., Başkal, T., Boran, K., and Boran, F. E., 2010, "Optimization of module, shaft diameter and rolling bearing for spur gear through genetic algorithm," *Expert Systems with Applications*, 37(12), pp. 8058-8064
- [5] Savsani, V., Rao, R. V., and Vakharia, D. P., 2010, "Optimal weight design of a gear train using particle swarm optimization and simulated annealing algorithms," *Mechanism and Machine Theory*, 45(3), pp. 531-541
- [6] Gologlu, C., and Zeyveli, M., 2009, "A genetic approach to automate preliminary design of gear drives," *Computers & Industrial Engineering*, 57(3), pp. 1043-1051
- [7] Pomrehn, L. P., and Papalambros, P. Y., 1995, "Discrete optimal design formulations with application to gear train design," *Journal of Mechanical Design (ASME)*, 117(3), pp. 419-424
- [8] Deb, K., and Jain, S., 2001, "Multi-speed gearbox design using multi-objective evolutionary algorithms," *Journal of Mechanical Design (ASME)*, 125(3), pp. 1-25.

Intentionally blank

MVM – International Journal for Vehicle Mechanics, Engines and Transportation Systems
NOTIFICATION TO AUTHORS

The Journal MVM publishes original papers which have not been previously published in other journals. This is responsibility of the author. The authors agree that the copyright for their article is transferred to the publisher when the article is accepted for publication.

The language of the Journal is English.

Journal *Mobility & Vehicles Mechanics* is at the SSCI list.

All submitted manuscripts will be reviewed. Entire correspondence will be performed with the first-named author.

Authors will be notified of acceptance of their manuscripts, if their manuscripts are adopted.

INSTRUCTIONS TO AUTHORS AS REGARDS THE TECHNICAL ARRANGEMENTS OF MANUSCRIPTS:

Abstract is a separate Word document, “*First author family name_ABSTRACT.doc*”. Native authors should write the abstract in both languages (Serbian and English). The abstracts of foreign authors will be translated in Serbian.

This document should include the following: 1) author’s name, affiliation and title, the first named author’s address and e-mail – for correspondence, 2) working title of the paper, 3) abstract containing no more than 100 words, 4) abstract containing no more than 5 key words.

The manuscript is the separate file, „*First author family name_Paper.doc*“ which includes appendices and figures involved within the text. At the end of the paper, a reference list and eventual acknowledgements should be given. References to published literature should be quoted in the text brackets and grouped together at the end of the paper in numerical order.

Paper size: Max 16 pages of B5 format, excluding abstract

Text processor: Microsoft Word

Margins: left/right: mirror margin, inside: 2.5 cm, outside: 2 cm, top: 2.5 cm, bottom: 2 cm

Font: Times New Roman, 10 pt

Paper title: Uppercase, bold, 11 pt

Chapter title: Uppercase, bold, 10 pt

Subchapter title: Lowercase, bold, 10 pt

Table and chart width: max 125 mm

Figure and table title: Figure _ (Table _): Times New Roman, italic 10 pt

Manuscript submission: application should be sent to the following e-mail:

mvm@kg.ac.rs ; lukicj@kg.ac.rs

or posted to address of the Journal:

University of Kragujevac – Faculty of Engineering

International Journal M V M

Sestre Janjić 6, 34000 Kragujevac, Serbia

The Journal editorial board will send to the first-named author a copy of the Journal offprint.

OBAVEŠTENJE AUTORIMA

Časopis MVM objavljuje originalne radove koji nisu prethodno objavljivani u drugim časopisima, što je odgovornost autora. Za rad koji je prihvaćen za štampu, prava umnožavanja pripadaju izdavaču.

Časopis se izdaje na engleskom jeziku.

Časopis *Mobility & Vehicles Mechanics* se nalazi na SSCI listi.

Svi prispeli radovi se recenziraju. Sva komunikacija se obavlja sa prvim autorom.

UPUTSTVO AUTORIMA ZA TEHNIČKU PRIPREMU RADOVA

Rezime je poseban Word dokument, „*First author family name_ABSTRACT.doc*“. Za domaće autore je dvojezičan (srpski i engleski). Inostranim autorima rezime se prevodi na srpski jezik. Ovaj dokument treba da sadrži: 1) ime autora, zanimanje i zvanje, adresu prvog autora preko koje se obavlja sva potrebna korespondencija; 2) naslov rada; 3) kratak sažetak, do 100 reči, 4) do 5 ključnih reči.

Rad je poseban fajl, „*First author family name_Paper.doc*“ koji sadrži priloge i slike uključene u tekst. Na kraju rada nalazi se spisak literature i eventualno zahvalnost. Numeraciju korišćenih referenci treba navesti u srednjim zagradama i grupisati ih na kraju rada po rastućem redosledu.

Dužina rada: Najviše 16 stranica B5 formata, ne uključujući rezime

Tekst procesor: Microsoft Word

Margine: levo/desno: mirror margine; unurašnja: 2.5 cm; spoljna: 2 cm, gore: 2.5 cm, dole: 2 cm

Font: Times New Roman, 10 pt

Naslov rada: Velika slova, bold, 11 pt

Naslov poglavlja: Velika slova, bold, 10 pt

Naslov potpoglavlja: Mala slova, bold, 10 pt

Širina tabela, dijagrama: max 125 mm

Nazivi slika, tabela: Figure __ (Table __): Times New Roman, italic 10 pt

Dostavljanje rada elektronski na E-mail: mvm@kg.ac.rs ; lukicj@kg.ac.rs

ili poštom na adresu Časopisa
Redakcija časopisa M V M
Fakultet inženjerskih nauka
Sestre Janjić 6, 34000 Kragujevac, Srbija

Po objavljivanju rada, Redakcija časopisa šalje prvom autoru jedan primerak časopisa.

MVM Editorial Board
University of Kragujevac
Faculty of Engineering
Sestre Janjić 6, 34000 Kragujevac, Serbia
Tel.: +381/34/335990; Fax: + 381/34/333192
www.mvm.fink.rs